# OBTAINING THE MOMENTUM DISTRIBUTION OF AN OBLATE BOSE-EINSTEIN CONDENSATE: A NUMERICAL ANALYSIS

by

Julia Franziska Maria Werra

---

A Thesis Submitted to the Faculty of the

OPTICAL SCIENCES

In Partial Fulfillment of the Requirements
For the Degree of

MASTER OF SCIENCES
WITH A MAJOR IN OPTICAL SCIENCES

In the Graduate College

THE UNIVERSITY OF ARIZONA

2011

## STATEMENT BY AUTHOR

This thesis has been submitted in partial fulfillment of requirements for an advanced degree at The University of Arizona and is deposited in the University Library to be made available to borrowers under rules of the Library.

Brief quotations from this thesis are allowable without special permission, provided that accurate acknowledgment of source is made. Requests for permission for extended quotation from or reproduction of this manuscript in whole or in part may be granted by the head of the major department or the Dean of the Graduate College when in his or her judgment the proposed use of the material is in the interests of scholarship. In all other instances, however, permission must be obtained from the author.

SIGNED: _____

## APPROVAL BY THESIS DIRECTOR

This thesis has been approved on the date shown below:

_____ _____

Brian P. Anderson
Assoc. Professor

Date

# ACKNOWLEDGMENTS

I would like to thank my advisor Brian Anderson, who always had an open door and would help me out with all the questions I had, Ewan Wright, who found the paper, that let me finish this thesis and who always had an open ear for my concerns with my simulations and spent numerous hours discussing my code with me.

I cannot say how thankful I am for all the people, that helped me with my Matlab code, especially in the beginning, when I just started working with Matlab, like Zach Newman and Jeffrey Brown. Zach, thank you so much for the time you spent teaching me the basic BEC theory and introducing me into the codes you had already written for BEC simulations.

I would like to thank all the people who read this thesis and checked on my English, like Jonathan Brand, Kyle Taylor, Greg Cohoon, Raisa Trubko and gave me a lot of insights on how to write an English essay.

Everybody working in the Academic Programs Office has been unbelievably helpful to me, starting from possibilities to print my thesis, over help with immigration and funding problems, up to the support I got to graduate from this program is such a short amount of time. I cannot stress enough how great of a job everybody in this office has done for me.

I would also like to thank the German Fulbright commission which sponsored my studies in the United States.

All my friends and my family, in the United States and in Germany, who always supported me and believed in me have to be mentioned here, however, there are far too many people to name, that I could not accomplish listing all of you.

# TABLE OF CONTENTS

LIST OF FIGURES . . . . . **6**

LIST OF TABLES . . . . . **8**

ABSTRACT . . . . . **9**

CHAPTER 1. INTRODUCTION . . . . . **10**
1.1. Fourier Transforms in Bose-Einstein Condensates . . . . . 11

CHAPTER 2. SIMULATING THE DYNAMICS OF A BEC . . . . . **13**
2.1. Ground State . . . . . 15
2.2. Introducing Vortices into a BEC . . . . . 17

CHAPTER 3. FOURIER-TRANSFORMATION OF A BEC . . . . . **21**
3.1. How to obtain a Fourier-Transformation of a BEC experimentally . . . . . 21
3.2. First Simulations with the Scaling Law . . . . . 29
3.2.1. Comparison of an Expansion with the Scaling Law . . . . . 29
3.2.2. Simulations for a Harmonic Trap . . . . . 30
3.2.3. Simulations for a Toroidal Trap . . . . . 34
3.3. Details of the Simulations . . . . . 36
3.3.1. Choice of Parameters . . . . . 37
3.3.2. Sensitivity of the Method . . . . . 38
3.4. More Data . . . . . 39

CHAPTER 4. USE OF THE DENSITY IN MOMENTUM SPACE OF A BEC . . . . . **46**
4.1. Coherence of a BEC . . . . . 46
4.1.1. Correlation Length . . . . . 47
4.1.2. Results for Non-Turbulent BECs . . . . . 50
4.1.3. Results for the Turbulent BECs . . . . . 52
4.1.4. Sensitivity Study for the Coherence length . . . . . 55
4.2. The Kinetic Energy . . . . . 58

TABLE OF CONTENTS—*Continued*

4.2.1. Kinetic Energies for Non-Turbulent BECs . . . . . 59
4.2.2. Kinetic Energies for Turbulent BECs . . . . . 60

CHAPTER 5. CONCLUSIONS . . . . . **61**

APPENDIX A. MATLAB CODE . . . . . **63**

APPENDIX B. DERIVATION OF THE SCALING LAW . . . . . **82**

APPENDIX C. THE DENSITY MATRIX . . . . . **85**

REFERENCES . . . . . **89**

# LIST OF FIGURES

FIGURE 2.1. Thomas-Fermi approximation of the ground state . . . . . 16
FIGURE 2.2. Ground State of a BEC . . . . . 17
FIGURE 2.3. Creation of pairs of vortices . . . . . 19
FIGURE 2.4. Wave-Functions $\phi$ . . . . . 20

FIGURE 3.1. Scheme of the Experimental Fourier-Transformation and its Implementation in the Simulation . . . . . 25
FIGURE 3.2. Expansion of BEC Originally in Toroidal Trap . . . . . 27
FIGURE 3.3. Toroidal Potential for Expansion . . . . . 28
FIGURE 3.4. Scaling Law . . . . . 30
FIGURE 3.5. Fourier Transform of a BEC with a vortex dipole . . . . . 32
FIGURE 3.6. Real-Space Distribution of BEC with 2 Vortices . . . . . 32
FIGURE 3.7. Comparison of Simulation to Fourier transform . . . . . 33
FIGURE 3.8. Fourier transform of toroidal wavefunction . . . . . 35
FIGURE 3.9. Evolution in Toroidal Trap . . . . . 36
FIGURE 3.10. Sensitivity to small inaccuracies of a BEC in Harmonic Trap to Experimental Procedure . . . . . 38
FIGURE 3.11. Sensitivity to small inaccuracies of a BEC in Toroidal Trap to Experimental Procedure . . . . . 39
FIGURE 3.12. Fourier Transform of Groundstate in Harmonic Trap . . . . . 40
FIGURE 3.13. Fourier Transform of BEC with 3 vortices in Harmonic Trap . . . . . 40
FIGURE 3.14. Fourier Transform of BEC with 4 vortices in Harmonic Trap . . . . . 41
FIGURE 3.15. BEC, after propagation in trap for $t_{\mathrm{hold}} = 1\ \mathrm{ms}$ . . . . . 42
FIGURE 3.16. BEC, after propagation in trap for $t_{\mathrm{hold}} = 51\ \mathrm{ms}$ . . . . . 43
FIGURE 3.17. BEC, after propagation in trap for $t_{\mathrm{hold}} = 5131\ \mathrm{ms}$ . . . . . 43
FIGURE 3.18. BEC, after propagation in trap for $t_{\mathrm{hold}} = 6158\ \mathrm{ms}$ . . . . . 44
FIGURE 3.19. BEC, after propagation in trap for $t_{\mathrm{hold}} = 10262\ \mathrm{ms}$ . . . . . 44
FIGURE 3.20. BEC, after propagation in trap for $t_{\mathrm{hold}} = 14362\ \mathrm{ms}$ . . . . . 45

FIGURE 4.1. Density matrix of state with 4 vortices . . . . . 48
FIGURE 4.2. Full-Width Half-Maximum of the density matrix . . . . . 48

LIST OF FIGURES—*Continued*

FIGURE 4.3. Time Evolution of Groundstate in Toroidal Trap . . . . . 54
FIGURE 4.4. Sensitivity Study for FWHM of state with 2 vortices . . . . . 56
FIGURE 4.5. Sensitivity Study for FWHM of state with 3 vortices . . . . . 56
FIGURE 4.6. Difference between FWHM for different times . . . . . 57
FIGURE 4.7. Sensitivity Study for FWHM of turbulent state . . . . . 57
FIGURE 4.8. Difference of FWHM between two time steps . . . . . 58
FIGURE B.1. Beam Parameters . . . . . 84
FIGURE C.1. Density matrix of state with 2 vortices . . . . . 85
FIGURE C.2. Density matrix of state with 3 vortices . . . . . 85
FIGURE C.3. Density matrix of state originally in toroidal trap at $t_{\mathrm{hold}} = 1\ \mathrm{ms}$ . . . 86
FIGURE C.4. Density Matrix of State originally in toroidal trap at $t_{\mathrm{hold}} = 51\ \mathrm{ms}$ . . 86
FIGURE C.5. Density Matrix of State originally in toroidal trap at $t_{\mathrm{hold}} = 1027\ \mathrm{ms}$ . 86
FIGURE C.6. Density Matrix of State originally in toroidal trap at $t_{\mathrm{hold}} = 5131\ \mathrm{ms}$ . 87
FIGURE C.7. Density Matrix of State originally in toroidal trap at $t_{\mathrm{hold}} = 6158\ \mathrm{ms}$ . 87
FIGURE C.8. Density Matrix of State originally in toroidal trap at $t_{\mathrm{hold}} = 10262\ \mathrm{ms}$ 87
FIGURE C.9. Density Matrix of State originally in toroidal trap at $t_{\mathrm{hold}} = 14362\ \mathrm{ms}$ 88

# LIST OF TABLES

TABLE 4.1. Full-Width Half-Maximum for the density matrix of non-turbulent BECs 50
TABLE 4.2. RMS for the density matrix of non-turbulent BECs . . . . . 52
TABLE 4.3. Full-Width Half-Maximum for the density matrix of turbulent BECs . . 53
TABLE 4.4. RMS for the density matrix of turbulent BECs . . . . . 55

# ABSTRACT

This thesis investigates the feasibility of an experiment to obtain the density distribution in momentum space of a dilute Bose-Einstein Condensate (BEC) using simulations. Mathematically, this is obtained with the Fourier transform of the wavefunction, however the phase information in current setups is not easily accessible which leads to the need for the development of an alternative experimental method. Methods are developed to analyze the Fourier transform of BECs held in harmonic or toroidal traps such that the resulting momentum distributions correspond to images that might be experimentally obtainable. In the method examined, after expanding the BEC two-dimensionally an optical or magnetic pulse is applied to remove the phase curvature that is accumulated during the process of expansion from the trap. To obtain the final Fourier transform the BEC is back-focused via three-dimensional propagation. This allows the extraction of information about the characteristics of a state of the BEC, such as the coherence length and the kinetic energy spectrum. Experimental parameters of this setup are discussed, concluding in an outlook on the use of the data obtained.

# Chapter 1
# INTRODUCTION

A dilute gas Bose-Einstein condensate (BEC) is a microscopic droplet of quantum fluid, that consists of atoms cooled down to temperatures very close to absolute zero. After its first prediction by A. Einstein in 1926 it took scientists until 1995 to observe a definite Bose-Einstein condensate for the first time [1], [2], [3]. BECs are used amongst others things to probe superfluidity, phase transitions and many-body physics.

In this thesis the achievement of a Fourier transform of a two-dimensional Bose-Einstein Condensate (BEC) is presented including the underlying theory and a study of experimental feasibility. In this context the word "two-dimensional" describes a trap that sufficiently confines the BEC in the z-direction so that the vortices created cannot bend or tilt with respect to the z-direction.

The (interacting) wavefunctions of all the particles contained in the system describes a given quantum system. In a Bose-Einstein condensate (BEC) every bosonic particle is in the exact same quantum-state, allowing one complex macroscopic wavefunction to describe the system. This wavefunction consists of the absolute value and a phase. The square of the absolute value represents the probability density of finding a particle at a certain position if normalized to 1. Otherwise this is the spatial density of atoms. The phase of the wavefunction contains information about the behavior in reciprocal space, also known as momentum space or $\boldsymbol{k}$-space. Experimentally only the density, which is the square of the absolute value is accessible except via interferometric techniques. To retrieve the information in $\boldsymbol{k}$-space out of the density in real space, an experiment that takes the Fourier transform of the wavefunction is required.

Similar experiments in optics are known. Using the formalism of the ABCD-Matrix,

one simply sets $A = D = 0$. For example, one can acquire the Fourier transform of a beam by sending it through a lens and measuring the intensity at the focal point.

The remaining part of **Chapter I** is about prior methods of obtaining Fourier transforms for different experimental setups and the reasons for taking Fourier transforms.

**Chapter II** covers the different ways to create ground states for BEC in harmonic traps and toroidal traps. Furthermore, several ways of introducing vortices into a BEC cloud are presented.

**Chapter III** proposes an experiment to create the density of the BEC in $\boldsymbol{k}$-space, $n(\boldsymbol{k})$. These experiments are Fourier transforms of states originally created in harmonic traps and any state whose potential is a superposition of a harmonic trap and another rotationally symmetric potential.

Finally, after the introduction of the basic theory, simulation codes and examples, **Chapter IV** discusses how this experiment is sensitive to changes of parameters and measurement uncertainties. This is performed by looking at different parameters, such as the coherence length, that can be extracted from the information obtained by Fourier-transforming the BEC.

The *Matlab* code that is used for the simulations in this thesis is in the **Appendix**.

## 1.1 Fourier Transforms in Bose-Einstein Condensates

Fourier Transforms have already been proven possible for experimental setups in which quasi one dimensional and quasi two-dimensional traps hold the BEC. These are different from the setup used at the Bose-Einstein Condensation lab at the University of Arizona.

In 2008 a Fourier transform of a one-dimensional BEC was achieved in Amsterdam [4]. The approach for this Fourier transform was in general the same lens approach this thesis is going to follow. "A strong axial harmonic potential"[1] acts like a lens on the one-

[1] p. 2, [4]

dimensional distribution. At the exact same time they turn off the trap, the BEC propagates until it is back in focus. At that point, they obtained a Fourier transformation and therefore a density distribution in momentum space. The BEC used in Amsterdam is quasi one-dimensional, whereas the setup at the University of Arizona allows for a highly oblate BEC. Due to the one-dimensionality of the Amsterdam experiment the pulse can be applied without prior expansion since the density decreases fast enough in the free expansion after the pulse was applied.

A Fourier transform was also applied to a two-dimensional BEC at the University of Colorado, Boulder [5]. A harmonic pulse was applied to the optically trapped BEC with $(\omega_r, \omega_z) = 2\pi \cdot (10, 1400)$ Hz at the same time that this trap was turned off. Therefore, the BEC was released into a remaining magnetic trap with trap parameters $(\omega_r, \omega_z) = 2\pi \cdot (5.2, 10.4)$ Hz. After a time $t = \frac{1}{4}\frac{2\pi}{\omega_r}$ the density distribution in $\boldsymbol{k}$-space is obtained. Although, this assumes a two-dimensional distribution, the shape of the potential leads to a lot of similarities compared to the one-dimensional case, especially the fast decrease of density when released from the trap. As discussed later, this is the key element that allows those experiments to obtain Fourier transforms and to be able to neglect non-linear terms.

Gaining knowledge about the Fourier transform of a BEC gives insight to characteristics of a BEC. One important characteristic is the coherence length, which is going to be discussed in chapter 4 in great detail. Most importantly, it describes the interference between atoms at two different positions. This allows for the conclusion on whether or not the phases are correlated.

The coherence length has been accessed before. In 2000 Bloch, Hänsch and Esslinger were able to measure the visibility of the atom cloud and therefore conclude on the coherence length [6]. For a one-dimensional BEC cloud they applied microwave-pulses with two slightly different frequencies that released atoms from the magnetically trapped into the untrapped state while forming matter wave beams. With this “double-slit” experiment the coherence length can be determined.

# Chapter 2

# SIMULATING THE DYNAMICS OF A BEC

As mentioned in the introduction the BECs analyzed in the Bose-Einstein Condensate Lab at the University of Arizona are approximated by a two-dimensional equation of motion, since in first order the wavefunction in x-y-direction uncouples from the wavefunction in z-direction

$$\psi\left(\boldsymbol{r},t\right)=\phi\left(\boldsymbol{\rho},t\right)\cdot\phi_z\left(z,t\right).$$

In the following we are going to use $\psi$ to describe the three-dimensional wavefunction, $\phi$ to describe the two-dimensional wavefunction, $\boldsymbol{r}$ and $\boldsymbol{\rho}$ to talk about the real coordinates in three and two dimensions respectively. Several books like [7] derive the equation of motion for a two-dimensional Bose-Einstein Condensate, which is known as the Gross-Pitaevskii equation (GPE):

$$\begin{aligned} i\hbar\partial_t\phi(\boldsymbol{\rho},t) &= \left[-\frac{\hbar^2}{2m}\boldsymbol{\nabla}_{\mathrm{T}}^2+W\right]\phi(\boldsymbol{\rho},t) \\ W &= \frac{1}{2}m\left(\omega_x^2x^2+\omega_y^2y^2\right)+U_2(N-1)\left|\phi(\boldsymbol{\rho},t)\right|^2 \end{aligned} \tag{2.1}$$

assuming the BEC is trapped in a harmonic potential with parameters

$$\omega=\omega_x=\omega_y=2\pi\cdot 8\ \mathrm{Hz}$$

$$\omega_z=2\pi\cdot 90\ \mathrm{Hz}.$$

The nonlinear term in the potential $W$ is the interaction energy and is obtained by integrating over the third dimension. Depending on the assumed shape this nonlinear term can have different coupling strengths, in the easiest model assumed for this thesis it is given as

$$U_2=\frac{U_0}{\sqrt{2\pi}l_z}$$

$$l_z = \sqrt{\frac{\hbar}{m\omega_z}}$$
$$U_0 = \frac{4\pi\hbar^2 a}{m}.$$

In the last equation the scattering length $a$ is specific for every atom. For Rubidium which is the element used in the lab it is given as

$$a = 5.5 \text{ nm}^1.$$

The equation of motion of a BEC wavefunction (2.1) is the basis to numerically simulate its dynamics. The computational work for this thesis was done in *Matlab*. To start with the simulations, one has to set up position($\boldsymbol{\rho}$) and momentum($\boldsymbol{k}$) space grids, that are conjugate spaces to be used in *Matlab*'s Fast Fourier Transformation algorithms[8].

If the real space grid lengths runs from $-\rho_{i,\max}$ to $\rho_{i,\max}$ with the number of sampling points $N_{\max}$, and $i \in x, y$ the spaces have to be constructed as follows:

$$d\rho_i = \frac{2\rho_{i,\max}}{N_{\max}}$$
$$\rho_i = -\rho_{i,\max}, ..., \rho_{i,\max} - dx$$

$$dk_i = \frac{2\pi}{2\rho_{i,\max}}$$
$$k_{i,\max} = \frac{\pi}{d\rho_i}$$
$$k_i = 0, -dk_i, ..., -k_{i,\max}, k_{i,\max} - dk_i, ..., dk_i.$$

After acquiring a working grid, the Schrödinger-equation (2.7) is implemented. As it is widely known, the Schrödinger-equation is solved by

$$\phi(\boldsymbol{\rho}, t) = e^{-\frac{i}{\hbar}\hat{H}\cdot t}\phi(\boldsymbol{\rho}, 0)$$

if the Hamiltonian is time independent or for times short compared to the dynamical time scales of the problem. With the kinetic energy operator diagonal in $\boldsymbol{k}$-space and the poten-

[1] [7], page 143

tial energy diagonal in $\boldsymbol{r}$-space, it would be useful to separate both parts, which is accomplished by the method of Trotter and Suzuki [9], even if those operators do not commute.

$$\exp\left(\hat{A}+\hat{B}\right)=\lim_{\beta\to\infty}\left(\exp\left(\frac{\hat{B}}{2\beta}\right)\exp\left(\frac{\hat{A}}{\beta}\right)\exp\left(\frac{\hat{B}}{2\beta}\right)\right)^{\beta} \tag{2.2}$$

Translating this into code implies the choice of a sufficiently small $dt=\frac{t}{\beta}$. One can apply the kinetic $\hat{K}$ and potential energy operator $\hat{W}$ once at a time, $\beta$ times. The potential energy operator contains the potential and the interaction Hamiltonian due to atom-atom interactions.

$$\left|\frac{A}{\beta}\right|,\left|\frac{B}{\beta}\right|<<1$$

leads to the following requirements for a time step $dt$:

$$\frac{\hbar}{m}k_{\max}^{2}\cdot dt<<1$$
$$\frac{W_{\max}}{\hbar}\cdot dt<<1.$$

With this condition using the *Split-Step-method* $\phi(\boldsymbol{\rho},t)$ can be calculated in $\beta$ steps, where $t=\beta\cdot dt$

$$\phi(\boldsymbol{\rho},t_{i+1})=\exp\left(-i\frac{\hat{W}}{2\hbar}dt\right)\cdot\mathrm{IFFT2}\left[\exp\left(i\frac{\hat{K}}{\hbar}dt\right)\cdot\mathrm{FFT2}\left(\exp\left(-i\frac{\hat{W}}{2\hbar}dt\right)\phi(\boldsymbol{\rho},t_{i})\right)\right] \tag{2.3}$$

given an initial state $\phi(\boldsymbol{\rho},t_0)$ and applying that procedure iteratively, from $t_i=t_0=0$ up to $t_i=t_{\beta-1}=t-dt$.

## 2.1 Ground State

Looking at the Gross-Pitaevskii equation (2.1), assuming $N$ is large and neglecting the kinetic energy term, which is equivalent to assuming very small values for the spatial derivatives of the wavefunction, the equation for a stationary ground state is written as

$$\left[V\left(\boldsymbol{\rho}\right)+U_{2}(N-1)\left|\phi_{\mathrm{tind}}\left(\boldsymbol{\rho}\right)\right|^{2}\right]\phi_{\mathrm{tind}}\left(\boldsymbol{\rho}\right)=\mu\phi_{\mathrm{tind}}\left(\boldsymbol{\rho}\right), \tag{2.4}$$

where $\phi(\boldsymbol{\rho}, t) = \mathrm{e}^{-i\frac{\mu t}{\hbar}}\phi_{\mathrm{tind}}(\boldsymbol{\rho}, t)$. This is called the Thomas-Fermi approximation and gives rise to a real wavefunction in the ground state:

$$|\phi_{\mathrm{tind}}(\boldsymbol{\rho})|^2 = \frac{2}{U_2(N-1)}(\mu - V(\boldsymbol{\rho})) = \frac{2\mu}{U_2(N-1)}\left(1 - \frac{\rho^2}{R_c^2}\right)\Theta(R_c^2 - \rho^2) \tag{2.5}$$

with the definition $R_C = \sqrt{\frac{2\mu}{m\omega}}$. An important variable in this wavefunction is the chemical potential $\mu$. This energy that is needed to add an additional particle to the cloud is extracted out of the normalization condition:

$$\int_0^\infty \mathrm{d}\rho 2\pi\rho\,|\phi_{\mathrm{tind}}|^2 = \int_0^{R_c} \mathrm{d}\rho 2\pi\rho \frac{2\mu}{U_2(N-1)}\left(1 - \frac{\rho^2}{R_c^2}\right) \stackrel{!}{=} 1 \tag{2.6}$$

which leads to:

$$\mu = \sqrt{\frac{2U_2(N-1)m\omega^2}{\pi}} \approx \sqrt{\frac{2U_2 N m\omega^2}{\pi}}$$

When plotting this wavefunction (compare figure 2.1) there is a problem at the values $\rho \approx R_c$. At those points the wavefunction becomes very steep and the derivative of the wavefunction very big. That, however, contradicts our assumption, that the kinetic energy is negligible in comparison to the potential energy.

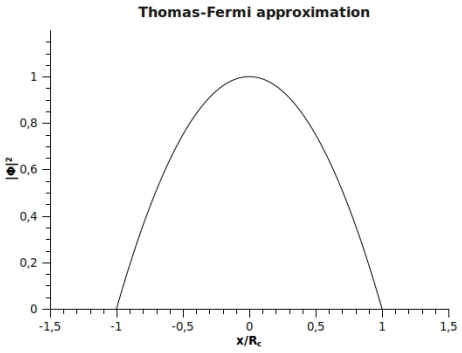


FIGURE 2.1. Thomas-Fermi approximation of the ground state

To avoid this contradiction between the result and the original assumptions, there are two additional steps needed when writing a code to create a working ground state. First eliminate these steep edges by developing the Thomas-Fermi solution (2.12) into Hermite-Gaussians. These are a complete and orthonormal set of functions and behave for $\rho$ close to $R_c$ like Gaussians and therefore have a small slopes at the points of interest.

However, they induce oscillations in the center of the ground state, which is not supported by the Thomas-Fermi Solution. Since those are small, the approximate initial

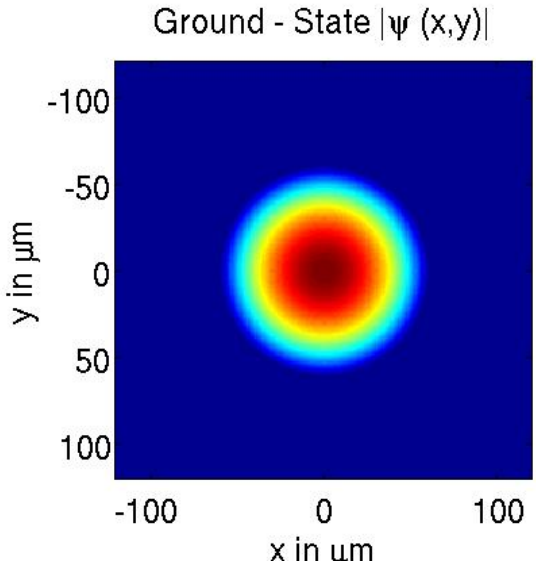


FIGURE 2.2. Density of the ground state of the BEC, where the colors depict the probability of finding a particle[3]at position $\rho$. The maximum density is displayed in red, whereas the minimum value is displayed in blue. The coding holds for all further plots of the density as well as the phase.

ground state solution needs to sit in the trap for about 100 ms with a damping term turned on, so that those oscillations are averaged over.

After those two steps (see code in Appendix A) we achieve a ground state that looks like the graph in figure 2.2. Starting at this point we are only assuming two-dimensional wavefunctions and states unless not otherwise stated. For simplicity the explicit notation $\phi(\boldsymbol{\rho})$ might be exchanged for $\phi$, equally for all the other variables depending on $\rho$.

## 2.2 Introducing Vortices into a BEC

The GPE can be used to simulate the dynamics of quantized vortices within the BEC ([7], chap. 9.1).

Multiplying equation (2.7) with the complex conjugated wavefunction and subtract-

[3]In the case of N particles, the probability of finding a particle within a small volume at position $\rho$ is equivalent to finding this percentage of the total number of the N particles at that position on a time average.

ing this modified equation by the complex conjugate of it leads to

$$\frac{\partial|\phi|^2}{\partial t} + \boldsymbol{\nabla} \cdot \left[\frac{\hbar}{2mi}\left(\phi^* \nabla\phi - \phi \boldsymbol{\nabla}\phi^*\right)\right] = 0. \tag{2.7}$$

With $n = |\phi|^2$ it is the continuity equation $\frac{\partial n}{\partial t} + \boldsymbol{\nabla} \cdot \boldsymbol{v} = 0$ and therefore

$$\boldsymbol{v} = \frac{\hbar}{2mi}\frac{(\phi^* \boldsymbol{\nabla}\phi - \phi \boldsymbol{\nabla}\phi^*)}{|\phi|^2}.$$

One can extract more information about the properties of the velocity, by writing $\phi = f \cdot e^{i\alpha}$, where $\alpha$ describes the phase of the complex wavefunction. This results in

$$\boldsymbol{v} = \frac{\hbar}{m}\boldsymbol{\nabla}\alpha. \tag{2.8}$$

The dependence on $\alpha$ is the reason for the possibility of introducing quantized vortices, since

$$\boldsymbol{\nabla} \times \boldsymbol{v} = 0$$

which leads to quantized circulation $\Gamma$

$$\Gamma = \oint \boldsymbol{v} \mathrm{d}\boldsymbol{l} = \frac{\hbar}{m} \cdot 2\pi l = \frac{h}{m} \cdot l. \tag{2.9}$$
$$l \in \mathbb{Z}$$

These quantized vortices carry angular momentum. A possibility to introduce vortices into a BEC without changing its angular momentum are vortex dipoles. This is a pair of vortices with opposite circulation and therefore opposite contributions to the BEC angular momentum. The resulting net angular momentum is therefore zero for a symmetrically placed vortex dipole. The vortices of a vortex dipole are moving under influence of each other, whereas the influence of other vortices is negligible.

One particular way to introduce vortex dipoles to a BEC was studied in detail at the Bose-Einstein Condensation Lab at the University of Arizona [10]. They showed in simulations and experiments, that after sweeping a BEC at a certain velocity along the x-axis through a laser beam, vortex dipoles arose. The experiment is done by applying a

laser beam on the left side of the center of the BEC, ramping it up until it has maximum intensity. Then the BEC is moved so that the laser potential is moved to the right side of the center of the BEC, while ramping the pulse-intensity down again. Since this setup can also be viewed as moving a laser beam through a cloud at rest, this description is going to be used in the following By introducing a velocity-component in x-direction, a local angular

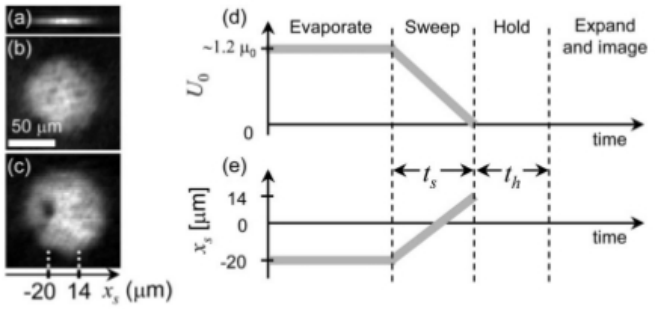


(a) Experiment to create a certain number of pairs of vortices, [10]

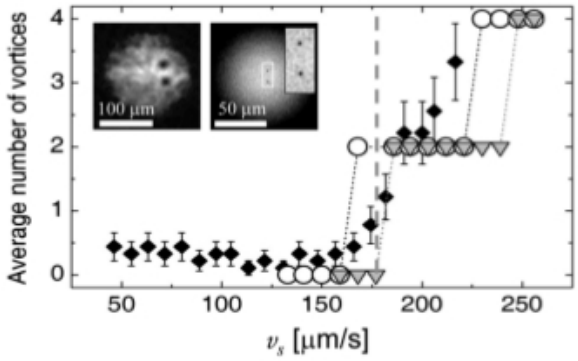


(b) This plot shows the dependence of the number of vortices created by a beam, that was swept through the BEC, on the speed of this beam [10]. The triangles are simulated values, the diamonds experimental averaged values. Simulations with less atoms and smaller Temperature (circles) result in more vortices for a given velocity.

FIGURE 2.3. Creation of pairs of vortices

momentum is introduced. Since the global angular momentum of the BEC is conserved, an even number of vortices is created. The number of created vortices depends on the number of atoms in the cloud, the diameter and intensity of the laser beam and, most importantly,

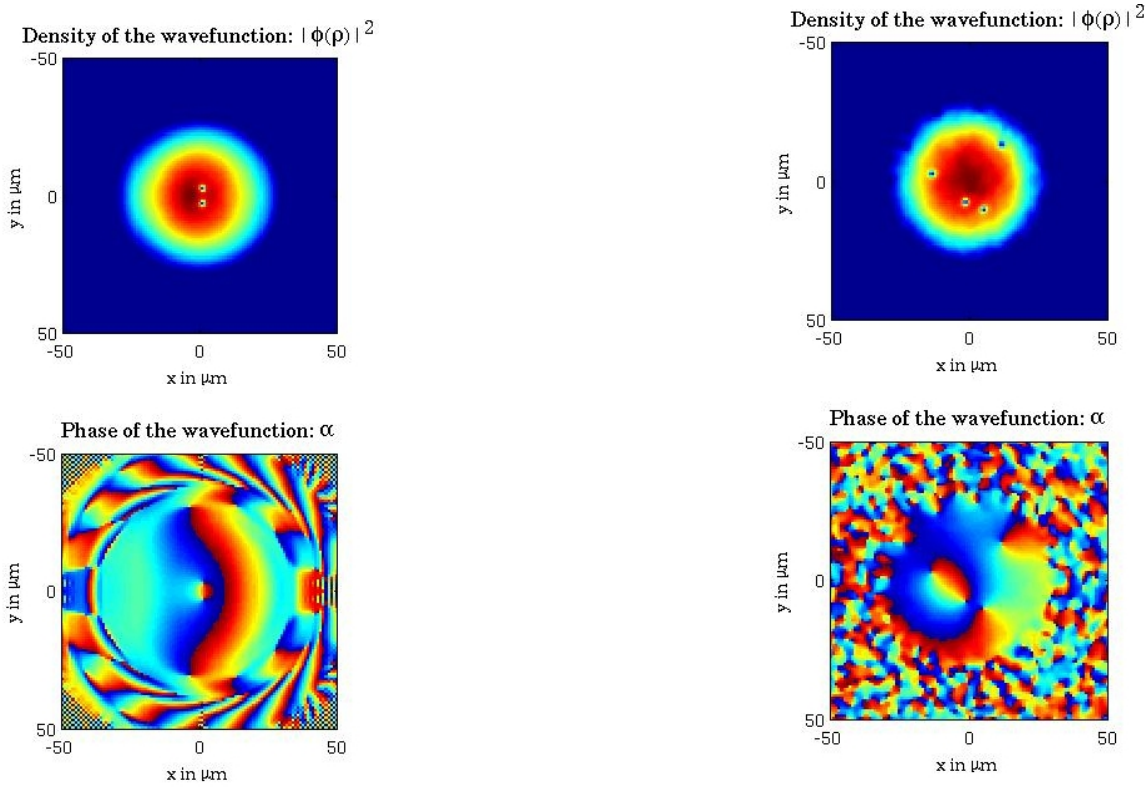


(a) Wave-Function with $v = 200\frac{\mu m}{s}$ and the procedure used in [10]

(b) Wave-Function created by a beam with its center at $\boldsymbol{r} = x_0$ with $\omega = \frac{v}{x_0}$ and same $v$.

FIGURE 2.4. The wave-functions $\phi(\rho)$ for different initial states. For better visibility of the vortices in the BEC only a part of the coordinate grid is displayed.

on the speed, with which one sweeps the beam through the cloud. Original plots of those experiments can be seen in figure 2.3.

Besides sweeping the beam linearly through a BEC, there are plenty of possibilities for the trajectory of the swept beam. These result in more complicated distributions of vortices. The non-uniform trajectory used to create states with more than a pair of vortices was a circle, starting at $(-x_0, 0)$, with the center at (0,0), while the beam was ramped down. Two of the states used to study the experimental Fourier transform can be seen in figure 2.4. Of those the right one is created with a linear movement of the beam whereas the left one is obtained after a circular movement.

# Chapter 3
# FOURIER-TRANSFORMATION OF A BEC

## 3.1 How to obtain a Fourier-Transformation of a BEC experimentally

There are several possibilities for obtaining a Fourier-Transformation of a BEC experimentally. First of all, one could allow the BEC to ballistically expand in free-space. This would work in practice if it was not for the nonlinear part, which can only be neglected when the non-linear part of the GPE is small in comparison to kinetic energy scales. One way to decrease the density is to expand the BEC. Assuming the density decreased very fast after releasing the BEC into three-dimensional space, it might be appropriate to realize a vanishing nonlinear term, which would lead to the following description of the propagation:

$$\phi(\boldsymbol{\rho}, t) = \frac{m}{2\pi i\hbar t'} \int_{-\infty}^{\infty} \mathrm{d}\boldsymbol{\rho} \exp\left(i\frac{m}{2\hbar t'}(\boldsymbol{\rho} - \boldsymbol{\rho'})^2\right)\phi(\boldsymbol{\rho'}, t),$$

where the z-direction of the wavefunction is still uncoupled from the wavefunction in the x-y-plane, since we start out in such a state.

However, this only leads to a Fourier transform if the assumption that the density has decreased sufficiently fast holds. Although this is possible, only releasing the BEC out of the trap in all three dimensions does not confirm whether it is an actual Fourier-Transformation and in practice the non-linear term cannot be neglected. Therefore this method does not present the best choice.

An experimentally realistic method for acquiring a Fourier transform is envisioned as follows: First, the wavefunction is released out of the x-y-trap, leading to an expansion in the x-y-direction, while the BEC is still two-dimensional. After a certain time $t$, a very short pulse is applied to imprint phase information; this pulse can either be optical or magnetic. This imprinted phase information cancels the curvature that is accumulated over the course of the experiments and allows the realization of the Fourier transform. At

the moment of the application of the pulse the magnetic trap in the z-direction is turned off so that the BEC is free to propagate in all three dimensions. Since the density is very low one can neglect the nonlinear term, after letting the BEC expand first in the x-y-plane. This assumption holds for all times until the BEC is focused in the x-y-plane at its Fourier transform, since the contraction in the x-y-direction that would normally increase the intensity can be compensated by an expansion in the z-direction.

The critical component is the two-dimensional expansion of the BEC at the beginning of the Fourier transform. This two-dimensional expansion allows for a "scaling law" as introduced in (3.1) below. Without the possibility to factorize the wavefunction in such a way with $\tilde{\phi}$ fulfilling the Schrödinger-equation of the BEC in a trap during the expansion, we would not be able to obtain this Fourier transform with all the interpretations of this method.

Mathematically the release and expansion of the BEC is described by solving the Schrödinger-equation

$$\begin{aligned} i\hbar\partial_t\phi(\boldsymbol{\rho},t) &= \left[-\frac{\hbar^2}{2m}\boldsymbol{\nabla}_{\mathrm{T}}^2+\frac{m}{2}\omega(t)^2\rho^2+U_2(N-1)\left|\phi(\boldsymbol{\rho},t)\right|^2\right]\phi(\boldsymbol{\rho},t), \\ \omega(t) &= \omega_0\Theta(t_0-t), \end{aligned} \tag{3.1}$$

where $t_0$, the time at which the BEC is released, is set to 0 for the rest of the thesis. With the choice of $\omega(t)$ in (3.1) we limit this first discussion to BECs originally confined by a harmonic potential. A discussion of the method for a toroidal trap is going to be in section 3.2.3 and in Appendix B.

As discussed in [11], in the two-dimensional case, (3.1) can be solved by this

**Ansatz:**

$$\phi_{\mathrm{lab}}(\tilde{\boldsymbol{\rho}},t)=\frac{1}{\lambda(t)}\exp\left(i\frac{m\tilde{\rho}^2\dot{\lambda}}{2\hbar\lambda}\right)\tilde{\phi}\left(\boldsymbol{\rho},\tau\right) \tag{3.2}$$

where $\rho$ and $\tilde{\rho}=\lambda(t)*\rho$ are two different coordinate systems, specifically the coordinate system in which the BEC is prior to any experiments and the coordinate system of the

expanded BEC. Furthermore $\phi_{\mathrm{lab}}$ describes the wavefunction of the BEC, that can be factorized in the three functions, $\lambda$ describes the expansion, the exponential function describes the built up curvature, and $\tilde{\phi}$ is a function we are going to develop an equation of motion for.

Plugging (3.2) into equation (3.1), a "new" Schrödinger-equation evolves accordingly

$$i\hbar\partial_\tau\tilde{\phi}(\boldsymbol{\rho},\tau) = \left[-\frac{\hbar^2}{2m}\boldsymbol{\nabla}_\rho^2 + \frac{m}{2}\omega_0\rho^2 + U_2(N-1)\left|\tilde{\phi}(\boldsymbol{\rho},\tau)\right|^2\right]\tilde{\phi}(\boldsymbol{\rho},\tau), \tag{3.3}$$

if $\lambda$ fulfills the following equation

$$\frac{\ddot{\lambda}}{\lambda} + \omega(t)^2 - \frac{\omega_0^2}{\lambda^4} \stackrel{!}{=} 0.$$

Since one only looks at times $t > t_0 = 0$, $\omega(t) = 0$ for this equation, the upper equation reduces to

$$\ddot{\lambda} = \frac{\omega_0^2}{\lambda^3} \tag{3.4}$$

$$\lambda(t) = \sqrt{1+\omega_0^2 t^2}. \tag{3.5}$$

Translating this result into code means first evolving the BEC for a time $\tau$ in the trap which determines the wavefunction at the points $\boldsymbol{\rho}$. This gives the wavefunction at positions $\tilde{\boldsymbol{\rho}}$. The upper equation holds for the scaling

$$\frac{\mathrm{d}t}{\lambda^2(t)} = \mathrm{d}\tau \Longleftrightarrow \omega_0\tau = \arctan(\omega_0 t).$$

After the successful expansion a pulse $\hat{M}$ is applied that consists of two parts. The first part is exactly large enough to cancel the phase curvature added during the expansion, whereas the second parts adds a curvature that is the negative of the curvature added by the following free-space propagation for time $t' = \tilde{t} - t$:

$$\begin{aligned}
\phi(\tilde{\boldsymbol{\rho}},\tilde{t}) &= \frac{m}{2\pi i\hbar t'}\int_{-\infty}^{\infty}\mathrm{d}\tilde{\boldsymbol{\rho}}'\mathrm{e}^{\left(i\frac{m}{2\hbar t'}(\tilde{\boldsymbol{\rho}}-\tilde{\boldsymbol{\rho}}')^2\right)}\phi(\tilde{\boldsymbol{\rho}}',t) \\
&= \frac{m}{2\pi i\hbar t'}\int_{-\infty}^{\infty}\mathrm{d}\tilde{\boldsymbol{\rho}}'\mathrm{e}^{\left(i\frac{m}{2\hbar t'}(\tilde{\boldsymbol{\rho}}-\tilde{\boldsymbol{\rho}}')^2\right)}\hat{M}\cdot\phi_{\mathrm{lab}}(\tilde{\boldsymbol{\rho}}',t) \\
&= \frac{m}{2\pi i\hbar t'\lambda(t)}\mathrm{e}^{\left(i\frac{m}{2\hbar t'}\tilde{\rho}^2\right)}\int_{-\infty}^{\infty}\mathrm{d}\tilde{\boldsymbol{\rho}}'\mathrm{e}^{\left(i\left(\frac{m}{2\hbar t'}+\frac{m\dot{\lambda}}{2\hbar\lambda}\right)\tilde{\rho}'^2\right)}\hat{M}\mathrm{e}^{\left(i\frac{m}{\hbar t'}\tilde{\boldsymbol{\rho}}\cdot\tilde{\boldsymbol{\rho}}'\right)}\tilde{\phi}\left(\frac{\tilde{\boldsymbol{\rho}}'}{\lambda},\tau\right).
\end{aligned} \tag{3.6}$$

This results in the following choice of $\hat{M}$:

$$\hat{M} = \exp\left(-i\eta(x'^2 + y'^2)\right) = \exp\left(-i\frac{m}{2\hbar}\left(\frac{1}{t'} + \frac{\dot{\lambda}}{\lambda}\right)\tilde{\rho}'^2\right). \tag{3.7}$$

With these equations we have constructed the foundation to understand the procedure to experimentally obtain the Fourier transform of any wavefunction[1]. First, we expand the wavefunction for a time $t$. The important parameter in this context is the scaling-factor $\lambda$, which not only tells us how much bigger the BEC is after the expansion, but also if the density has reduced enough to neglect the nonlinear term. The wish to be able to neglect that term is the main reason why one expands the BEC.

[1]For a graphical presentation of the complete procedure, see Fig. 3.1

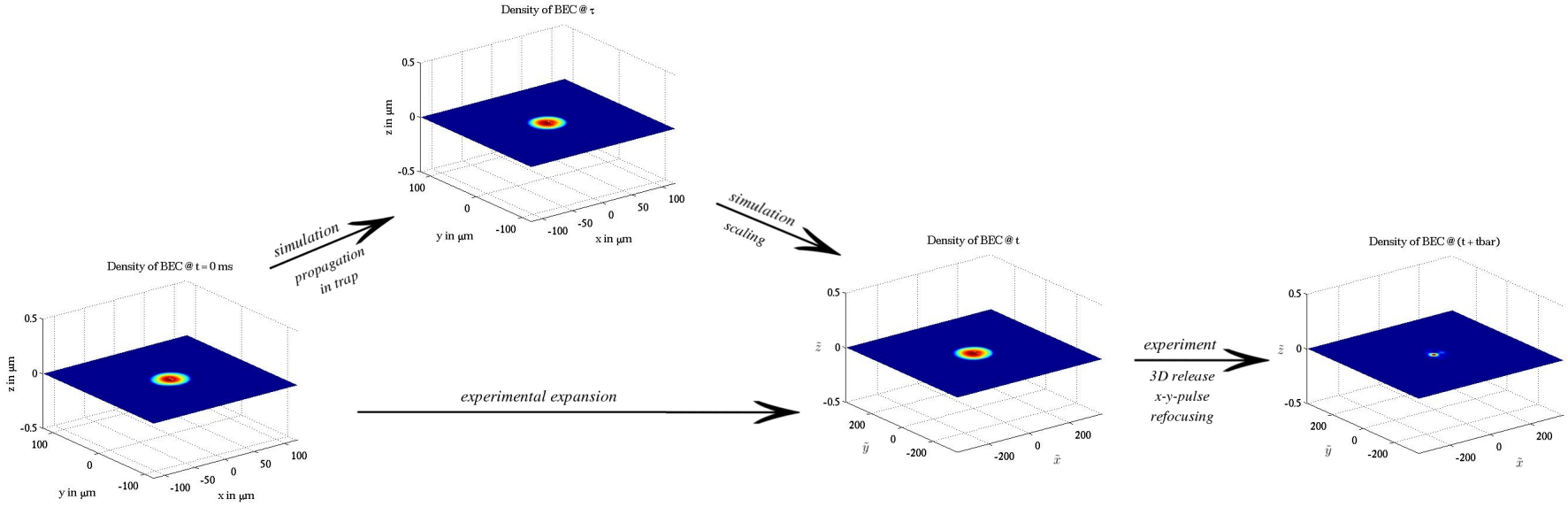


FIGURE 3.1. Scheme of the Experimental Fourier-Transformation and its Implementation in the Simulation

Another point to note is the way the expansion is written. There are several advantages in choosing the Ansatz (3.2):

1. It is a "scaling law", which means that in the simulation performed there is no need to change the size of the grid. One only has to rescale the whole BEC after propagation for some time in the trap in order to determine the actual BEC wavefunction.

2. It is easier to grasp the physical consequences for the BEC due to expansion. First of all, the BEC is expanded by a factor $\lambda$, which relates the size of the BEC after the two-dimensional expansion with the time of the expansion and leads to a quantitatively controllable size. Second, there is an additional evolution of the original BEC in a harmonic trap. For a BEC originally trapped in a harmonic trap, one can choose $\omega_0$ for the original trap frequency. As can be seen in Appendix B, the introduction of $\omega_0$ does not depend on the trap the BEC was originally confined in, so this description is valid for any trap.

3. The last important detail is that in the method investigated in this thesis one takes the Fourier transform of $\tilde{\phi}$. That implies, that one does not take the Fourier transform of the original wavefunction but of the wavefunction at a later time $\tau$ in the harmonic trap. For any BEC in a harmonic trap, it has just to be taken into account and is not a major disadvantage.

The "scaling-law" that describes a two-dimensional expansion independent of the potential in which the BEC was trapped prior to release allows an interpretation of the Fourier transform obtained. However, this interpretation only holds for harmonic traps. To interpret the final state for a BEC released out of arbitrary rotationally symmetric traps the procedure needs to be adjusted. An example of this situation is given in figure 3.2, where a BEC originally in a toroidal trap is expanded by the proposed method. However, the state that is later Fourier-transformed is not mapped back onto any state in the time evolution of the BEC in

the toroidal trap. This is of no interest when aiming to obtaining the Fourier transform of the BEC in the original trap.

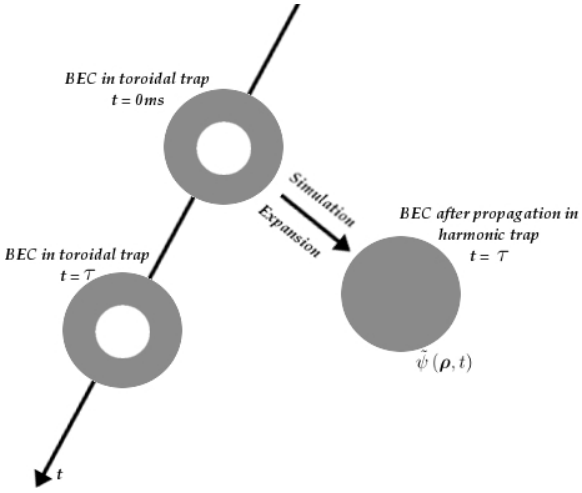


FIGURE 3.2. Expansion of BEC Originally in Toroidal Trap

Therefore we need to determine an alternate procedure. In the lab, the two traps used are the harmonic trap, for which we already have elaborated a working procedure to simulate a Fourier transform technique or the toroidal trap, which is a superposition of a harmonic trap and a blue-detuned (thus repulsive) Gaussian laser beam with amplitude $B_0$ and width $w_0$. Turning this potential completely off results in an expansion that is equivalent to an evolution in a harmonic trap. If the evolution is to be equivalent to an evolution in a toroidal trap, the Gaussian beam must remain turned on during the simulation in the trap[2]. However, since the BEC expands in the real experiment, one has to modify $B_0 \rightarrow B(t)$ and $w_0 \rightarrow w(t)$ to fulfill equation (B.3). As proved in Appendix B

$$B(t) = \frac{B_0}{\lambda(t)^2} \qquad\qquad w(t) = w_0 \cdot \lambda(t)$$

which leads to the potentials at different times seen in figure 3.3. In other words, the actual experiment would proceed by ramping off the beam during expansion and the scaling law in the computational procedure must do the same.

Finally, to obtain a real Fourier transform of either state, one has to translate the real-space coordinates into its equivalent $\boldsymbol{k}$-space coordinates and also the intensity of the final wavefunction:

[2]Discussion with Prof. Ewan M. Wright

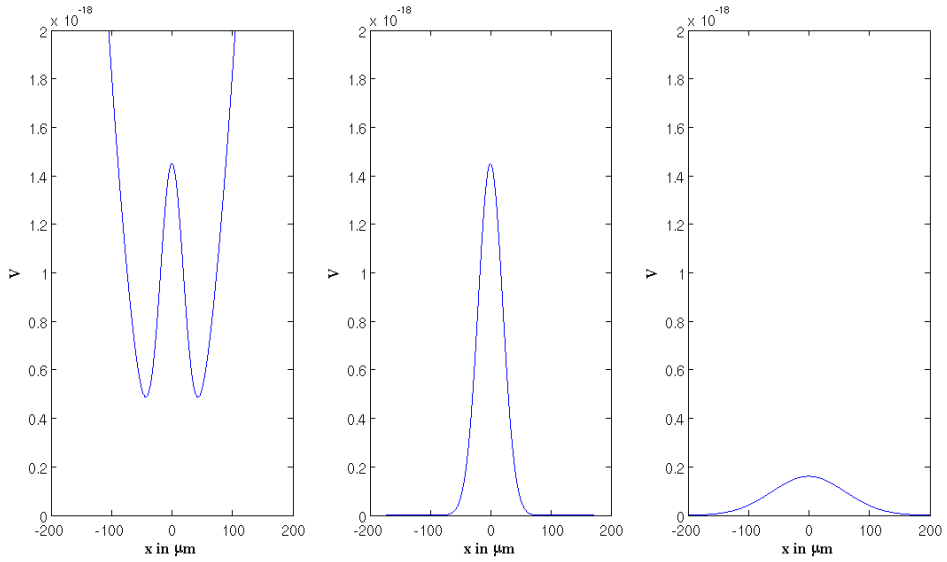


FIGURE 3.3. The toroidal potential at different times: originally the trap has a cross section of potential energy that looks like the picture on the left. To start the expansion of the BEC, one has to turn of the harmonic part of the potential. During the expansion, the Gaussian beam parameters are always to be changed, since after the expansion the beam looks like the picture on the right hand side

1. First of all, one has to translate $\tilde{x}_j \to k_j$ with $j \in x, y$. The wavefunction is separable for the x- and the y-dimension as $\phi(x, y) = \phi(x) \cdot \phi(y)$:

$$\begin{aligned} \phi(\tilde{x}_j, \tilde{t}) &\propto \int_{-\infty}^{\infty} \mathrm{d}\tilde{x}'_j \mathrm{e}^{\left(i\frac{m}{\hbar t'}\tilde{x}_j \cdot \tilde{x}'_j\right)} \tilde{\phi}\left(\frac{\tilde{x}'_j}{\lambda}, \tau\right) \\ &= \lambda(t) \int_{-\infty}^{\infty} \mathrm{d}x'_j \mathrm{e}^{\left(i\frac{m\lambda(t)}{\hbar t'}\tilde{x}_j \cdot x'_j\right)} \tilde{\phi}\left(x'_j, \tau\right) \\ &\to k_j = \frac{m\lambda(t)}{\hbar t'}\tilde{x}_j \end{aligned} \tag{3.8}$$

   where $k_i$ is in the original coordinate system. This results in the above equation simply being a Fourier transform of the evolved wavefunction at $\tau$.

2. The next task is to scale the intensity. Here, we are only interested in the absolute value since in experiments only the density is accessible from measurements if coherence is not considered. Using the factors from equation (3.6) and the additional

$\lambda(t)$ for every dimension (3.8), the prefactor for the Fourier transform yields

$$\mathcal{N} = \frac{m\lambda}{2\pi i\hbar t'}$$

Translating a sum into an integral, is done by the following transformation

$$\frac{1}{\Delta x^2}\int \mathrm{d}^2x \longleftrightarrow \sum$$

To obtain a corresponding Fourier transform to *Matlab*'s Fast Fourier Transform[3] from eq. (3.8), the wavefunction is multiplied by

$$\frac{1}{\mathcal{N}\Delta x^2}.$$

In the experiment only the optical density of the BEC is measured, which is divided by $|\Delta x^2\mathcal{N}|^2$.

## 3.2 First Simulations with the Scaling Law

### 3.2.1 Comparison of an Expansion with the Scaling Law

Using the results of the section above facilitates the implementation of a code for the expansion. However, it has still to be shown, that in code the two ways of expanding a BEC (scaling law versus expansion based on the split-step propagation) produce the same result.

As a first step, the BEC state was expanded with two vortices in it. This expansion holds some difficulties. First of all, one would like to use a grid as small as possible to increase the speed of the simulation, on the other hand, it has to be big enough that the BEC does not see the boundaries and therefore does not backscatter. To achieve these two conditions, one needs to change the size of the grid during the simulations.

As an approximation, the BEC was inserted into the center of a bigger grid. Since this was performed, when the BEC was still small enough chances were good that even with

[3] *Matlab2010b* defines their FFT in their help as $Y_{p+1} = \sum_{j=0}^{m-1} w_m^{jp} X_{j+1}$ with $w_m = \mathrm{e}^{-\frac{2\pi i}{m}}$.

only applying zero values to the new points in the grid minimal backscattering or other interferences would occur.

As one can see in Figure 3.4, this method is sufficient to compare the numerical expansion with the scaling law qualitatively. Assuming an initial state that is a nearly two-dimensional state, the scaling law will always give better quantitative results since there is less numerical inaccuracy involved with that procedure.

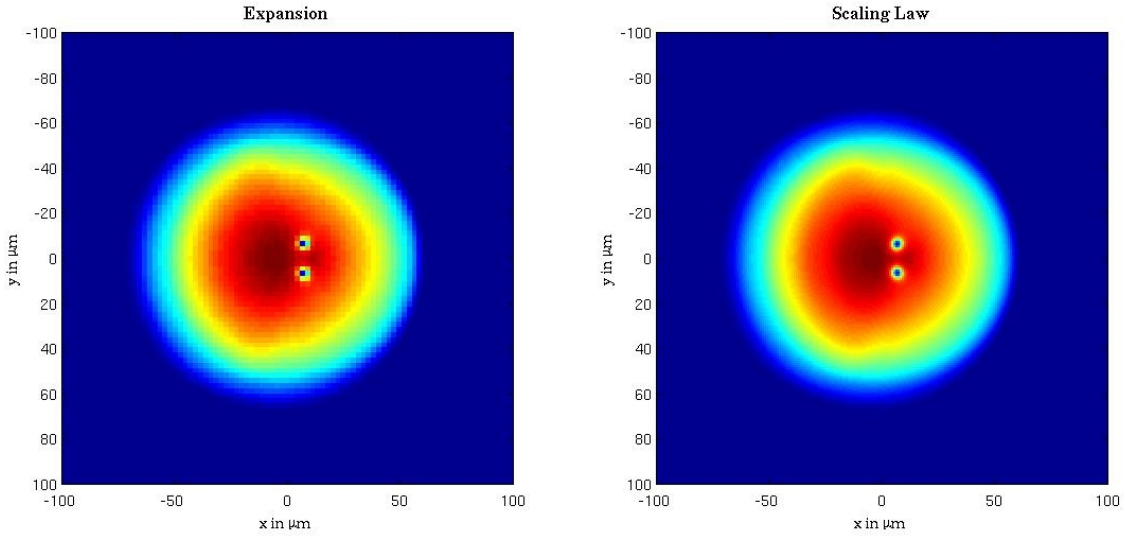


FIGURE 3.4. Density of the wavefunction, after split-step expansion on the left hand side in a larger grid and split-step propagation in the trap followed by scaling on the right hand side.

### 3.2.2 Simulations for a Harmonic Trap

The first test for the theory and the scaling law is the Fourier transform of a BEC in a Harmonic trap with a pair of vortices in it. It is slightly more complicated than the pure ground state with small scales in the center, but it is not turbulent. This means it is smooth over a wide range.

Three different situations should be considered in the simulations. To describe these

we use the following terminology

- *Calculated Fourier transform:* This is a Fourier transform carried out numerically by *Matlab*. Its use is to compare the simulated experiment to the expected result.

- *time t:* As can be seen in Chapter II the time $t$ is used here to describe the real time, during which the expansion takes place in the experiment. Any Fourier transform at a time $t = 0\ \mathrm{ms}$ is the transform of the original state one wants to take the Fourier transform of. Any other time $t$ gives information on how long that state would be expanded in the experiment prior to refocusing to achieve the same result.

- *time $\tau$:* This time is the corresponding simulation time. As pointed out in the previous chapter an expansion for time $t$ is equivalent to a propagation for time $\tau$ in an appropriate trap and a later expansion. Calculating a Fourier transform of a BEC at a time $\tau$ is therefore always a Fourier transform of the propagated but not yet scaled wavefunction.

- *Focused Wave Function:* This is the simulation of the real experiment. The original BEC was expanded, a pulse was applied while releasing the state also in the z-direction and it was back focused to the reconstruction of the Fourier transform.

Keeping this terminology in mind, figure 3.5 shows this set of Fourier transforms. In this picture the wavefunctions were magnified. In all the following graphics of Fourier transforms only the magnified wave are displayed, the actual size that depends on the expansion and back focusing time can be told by the labels of the axis. Furthermore figure 3.6 compares the wavefunction at time $t = 0\ \mathrm{ms}$ and the further propagated BEC at time $\tau$.

One can see, how good the numerical Fourier transform at time $\tau$ and the simulated experiment match up. The only fact one has to keep in mind is that those simulations

[5] As can be seen in Appendix C, in the code the variable *tbar* was used for $t'$.

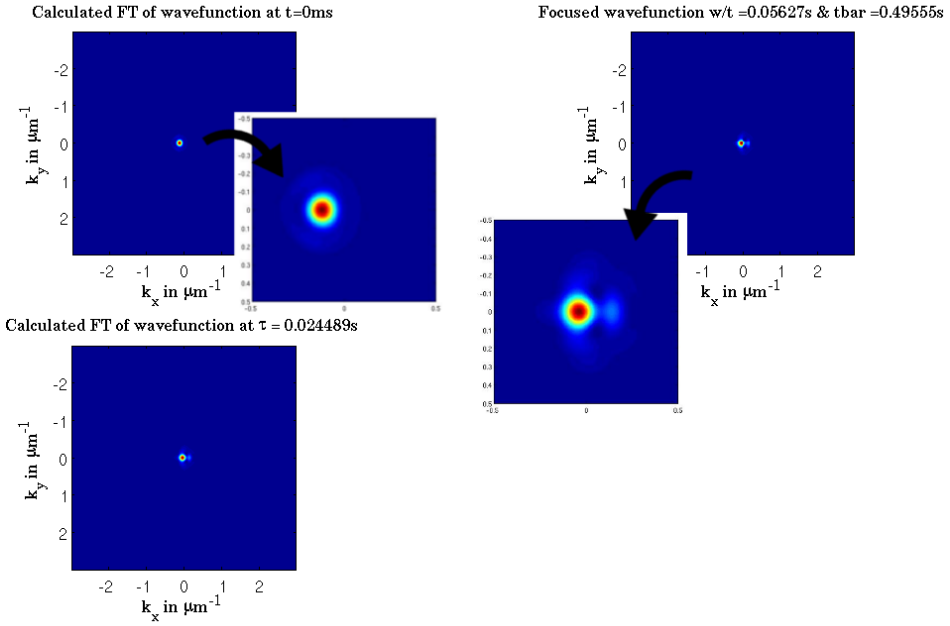


FIGURE 3.5. Fourier Transform of the original state and the Fourier Transform of a later state of a BEC with a vortex dipole[5]

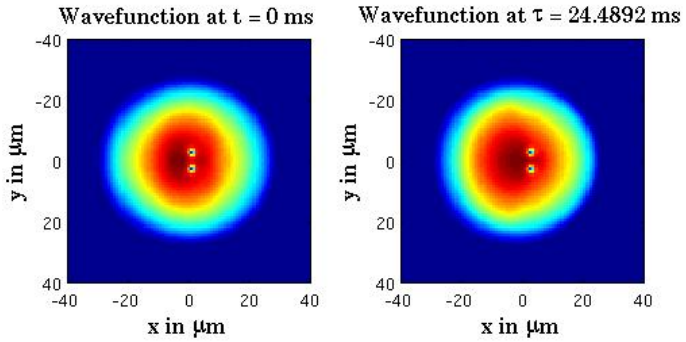


FIGURE 3.6. Real-space distribution of a BEC with 2 vortices at different times in harmonic trap.

are done without a damping term. This damping term implies that one would obtain the Fourier transform at a slightly earlier time and the Fourier transform might not be as perfect. However, since damping is negligible on these time scales in the real experiment is it is not necessary to include damping into this discussion. As we will later see (chapter IV) parameters we would like to extract from the Fourier transform do not change much for a state at different times in the trap and therefore it is negligible.

To facilitate a comparison between the direct Fourier transform of the initial state and the full experimental procedure of expansion in two dimensions and refocusing in two dimensions one can look at a cut along $y = 0\,\mu\mathrm{m}$. As one can see in figure 3.7 the simulation as well as the numerically computed Fourier transform look the same when one considers the necessary scaling as discussed in section 3.1.

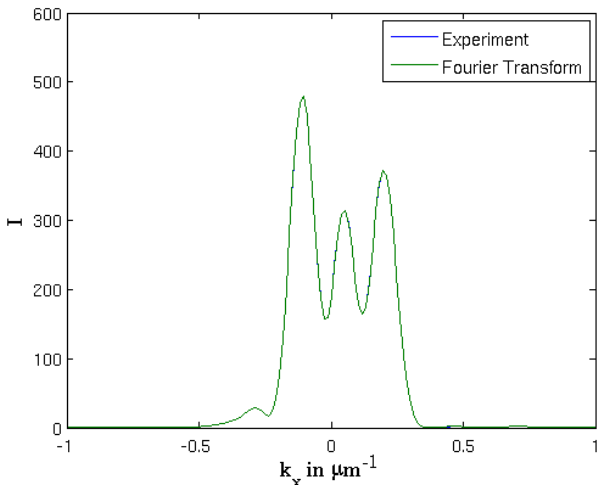


FIGURE 3.7. Cut along x-axis for the numerically calculated Fourier transform (called "Fourier Transform") and the simulation of the experiment (called "Experiment") for a state with 4 vortices.

### 3.2.3 Simulations for a Toroidal Trap

As described in section 3.1 one can use the scaling law to develop an expansion procedure for a BEC in a toroidal trap. This is used to take the Fourier transform of a state at a later time in the toroidal trap, but it also yields another feature. To see vortices in the real experiment one expands the BEC. Without the information of the scaling law about how to manipulate the parameters of the toroidal trap

$$V = B(t) \cdot \exp\left(-\frac{x^2+y^2}{w(t)^2}\right) + \frac{m}{2}\omega \cdot \left(x^2+y^2\right)$$

$$\boxed{\begin{aligned} \lambda(t) &= \sqrt{1+\omega_0^2 t^2} \\ B(t) &= \frac{B_0}{\lambda(t)^2} \\ w(t) &= w_0 \cdot \lambda(t) \end{aligned}}$$

one cannot look at vortices in a toroidal density distribution but always has to first remove the central Gaussian laser barrier then expand the BEC. One possibility of changing these parameters experimentally and allowing for an expansion of a toroidal density distribution is changing the size of the laser beam while decreasing the intensity. This could be experimentally achieved by shifting the plane in which the beam is focused.

This is a handy result however, it is not the main aspect of this thesis that rather focuses on the different Fourier transforms. In the case of the toroidal trap, we could work with several turbulent data sets, that correspond to experiments done in the BEC lab at the University of Arizona. These states are produced by starting with a BEC in a toroidal trap and moving the center laser beam in a very small circle through the trap until it returns to its original position in the center of the trap after $t = 333\,\mathrm{ms}$. As a first example a state was chosen where the BEC has been sitting in the trap for the time ($t_{\mathrm{hold}} = 1027\,\mathrm{ms}$) after the stirring process. Applying the experimental method presented above to this state leads to the Fourier transform in figure 3.8. As seen in the Harmonic Trap, the numerical Fourier

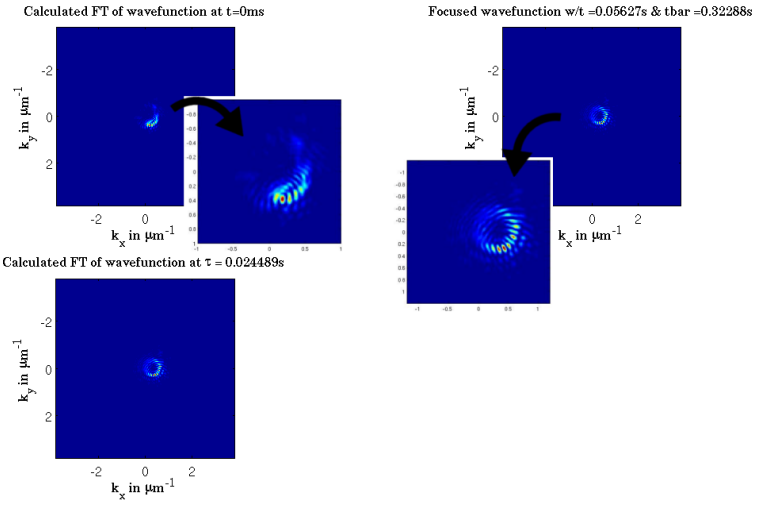


FIGURE 3.8. Fourier transform of wavefunction that was kept in toroidal trap after the creation of vortices for $t_{\mathrm{hold}} = 1027\ \mathrm{ms}$

transform matches exactly the simulated experiment. The scaling of the k-space coincides, a check of the scaling of the intensity does not yield additional insight.

Since the code to create the states differs from the two-dimensional Ansatz used for this thesis the trap parameters needed to further propagate the BEC in the trap do not match the original trap parameters perfectly. Additionally it was realized too late, that the width for the laser beam used in this thesis varied by a factor of $\sqrt{2}$ from the value originally used to create those states. Therefore the state at a time $\tau$ in real-space looks different in size and intensity from the original state, but general features are preserved. The states before and after the evolution in the trap are shown in figure 3.9. To compare the results obtained in this thesis with a real experiment the results are not fully quantitatively accurate. For a study of feasibility they are, however, sufficient as long as one keeps this discrepancy in mind.

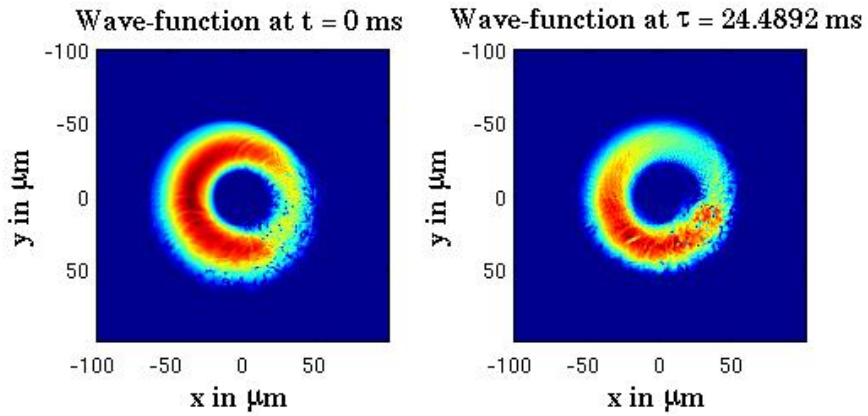


FIGURE 3.9. Evolution in Toroidal Trap

## 3.3 Details of the Simulations

Before executing any real experiment, these simulations need to be discussed in greater detail. Performing these simulations one is able to choose quite a few parameters freely, however, they influence each other. Since one can only control the experimental parameters up to a certain accuracy, the sensitivity of this method is an important feature. The disadvantage of this method is that there is no possibility in deciding experimentally when the Fourier transform is obtained, besides from calculating the refocusing time needed from the knowledge of the pulse strength. In contrast to the Fourier transform of a beam by a lens, this Fourier transform cannot be found at the focus for the nonlinear parts in the potential. Also, the change between states at different times could be minimal right before and after the exact Fourier transform, but that is not the case either. That shows, how important it is to know about the sensitivity of this transform to be able to estimate whether or not this

experiment is feasible.

### 3.3.1 Choice of Parameters

Concentrating on the parameters one needs to choose, there are several things to adhere to:

- $\lambda$: As discussed in the previous section, one need to choose $\lambda$ big enough to be able to neglect nonlinear interactions and small enough, that the state really Fourier-transformed is as close as possible to the original state that is supposed to be Fourier-transformed. We choose $\lambda = 3$.

- *Size of the Fourier transform:* One rather important thing to keep in mind is that in doing the experiment, one would like to be able to look at the BEC without the necessity to expand it further when it is at the focus. This is based on everything we learned about the further propagation of a BEC while undergoing expansion.
  In the simulations it is pretty easy to make sure that one ends up with a reasonable resolution and size. Since we can numerically calculate the Fourier transform of the propagated state one knows the size of the BEC at the time of "focus" before starting, and can choose
  $$k'_{x,\max} = \frac{m}{\hbar t' \lambda} x_{\max} \tag{3.9}$$
  and since we can determine $k'_{x,\max}$ in the simulations it is easy to choose ***t'*** accordingly. When starting out in the experiment without knowing the eventual size of the Fourier transform in k-space it might be preferable to try a few different $t'$. The choice of different $t'$ is experimentally implemented by choosing different pulse strengths.
  One important limit to the length of $t'$, which is, as seen in eq. (3.9), directly proportional to the size of the $\boldsymbol{k}$-space is the signal-to-noise ratio. Since it should not become to big, especially for a very small $\boldsymbol{k}$-space, $t'$ would necessarily become

huge. This follows from the need of a reasonable final BEC size, which will obviously be bigger for same back-focusing times $t'$ when possessing a bigger $\boldsymbol{k}$-space. Therefore it is especially hard to experimentally obtain a Fourier transform of a very smooth state, as for example the ground state, and much easier for turbulent states. The targeted states are mainly turbulent state, which results in this being less of an issue. Another possibility to solve this issue is to use better imaging optics so that the real-space and therefore the momentum space can be resolved better. All these possibilities need to be addressed when implementing the experiment, however, simply expanding the obtained momentum distribution is not the solution, since we have seen that an expansion leads to additional evolution of the BEC.

In the following data, one can, however, notice pretty big back-focusing times for the "easier" states, which can be explained and neglected with this discussion.

### 3.3.2 Sensitivity of the Method

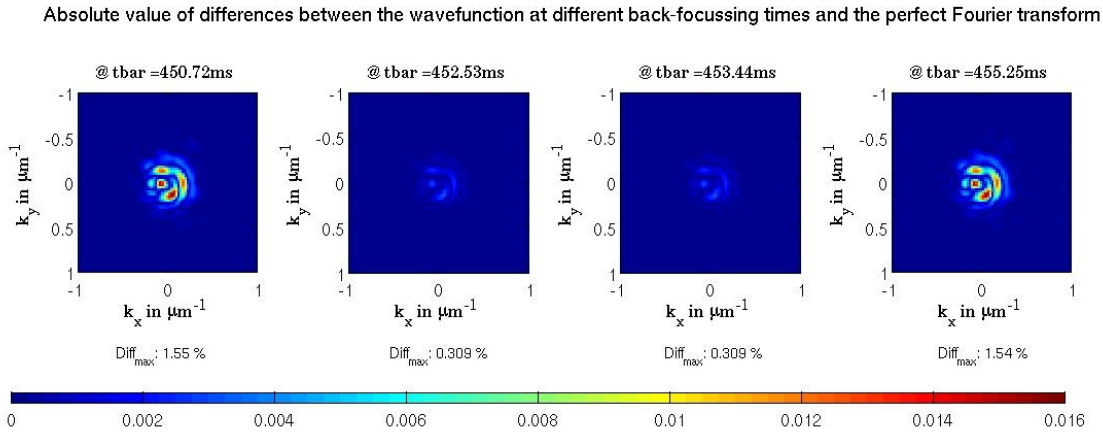


FIGURE 3.10. Difference between the Fourier transform of a state with 4 vortices and off sets of the back focusing time $t' = \mathrm{tbar}$.

As mentioned previously, one important factor that has to be considered when discussing the feasibility of the experiment is the sensitivity of this way of taking the Fourier

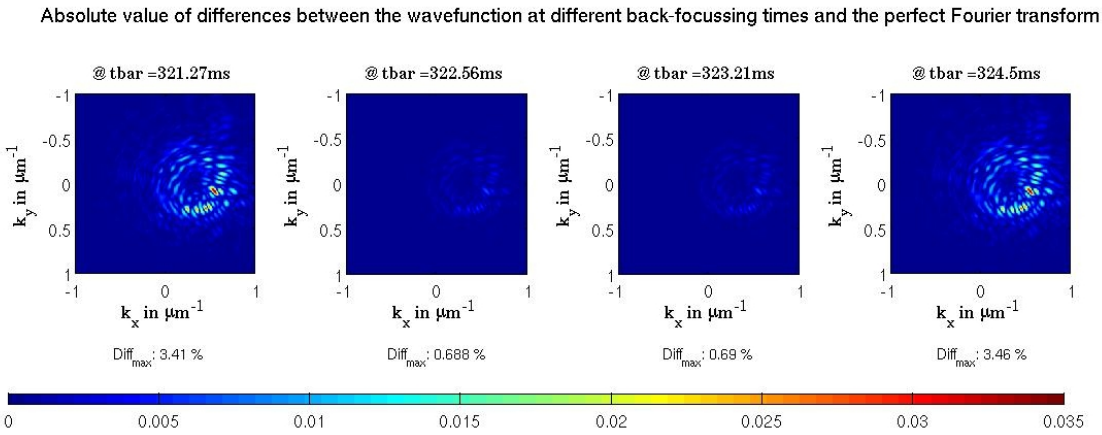


FIGURE 3.11. Difference to Fourier transform for slightly off set back-focusing times

transform. There are different parameters one can look at when making a judgment about the sensitivity. We will come back to the sensitivity of several parameters that one can obtain from $n(\boldsymbol{k})$ when talking about those parameters. However, right now, we would simply like to look at the difference between the intensity distribution at the time when one obtains the Fourier transform, and at times slightly earlier and later. To have a more relative measure of the differences, we plotted the results in the figures 3.10 and 3.11 normalized by the peak value of the Fourier transform and also pointed out the maximum absolute difference. For this study we used a state with 2 vortex pairs and another state in a toroidal trap.

## 3.4 More Data

Besides the two examples used earlier in the thesis to really investigate the properties of the Fourier transform, several more examples can be shown.

First, it is interesting to look at the Fourier transforms of BECs in a harmonic trap with different numbers of vortices (figures 3.12 - 3.14): Besides the state with a pair of vortices, which was already discussed in an earlier section, there are two more states with a number of vortices in them. The method to produce those two states is best described,

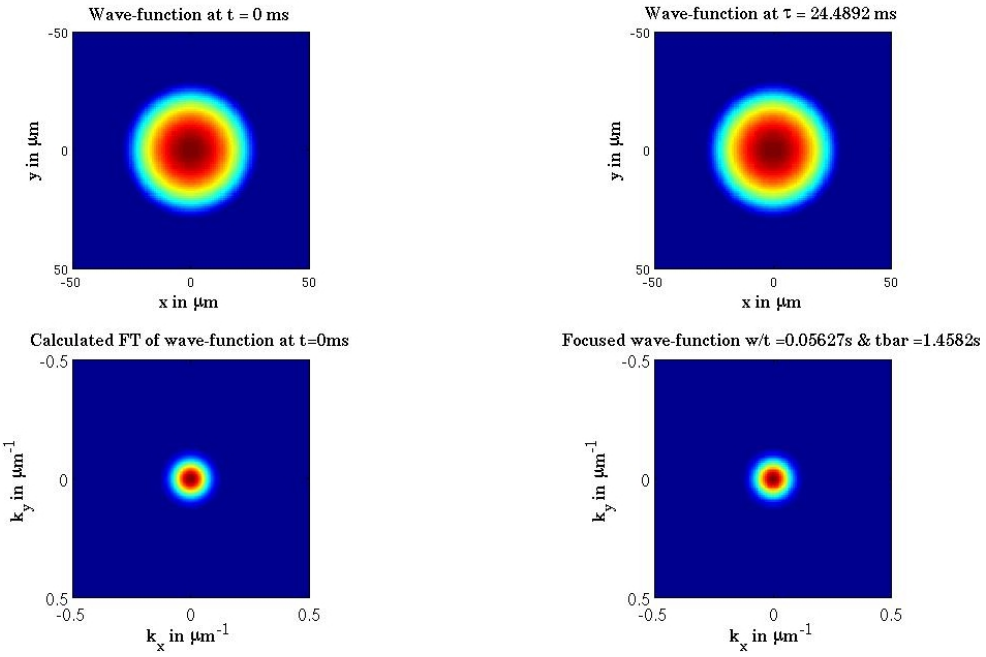


FIGURE 3.12. Fourier Transform of Groundstate in Harmonic Trap

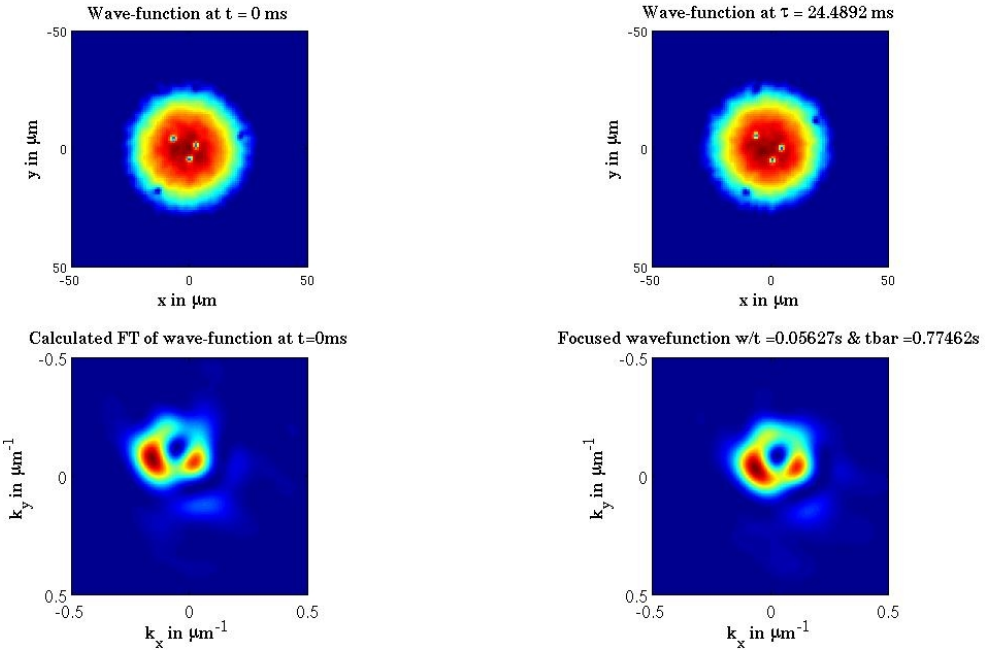


FIGURE 3.13. Fourier Transform of BEC with 3 vortices in Harmonic Trap

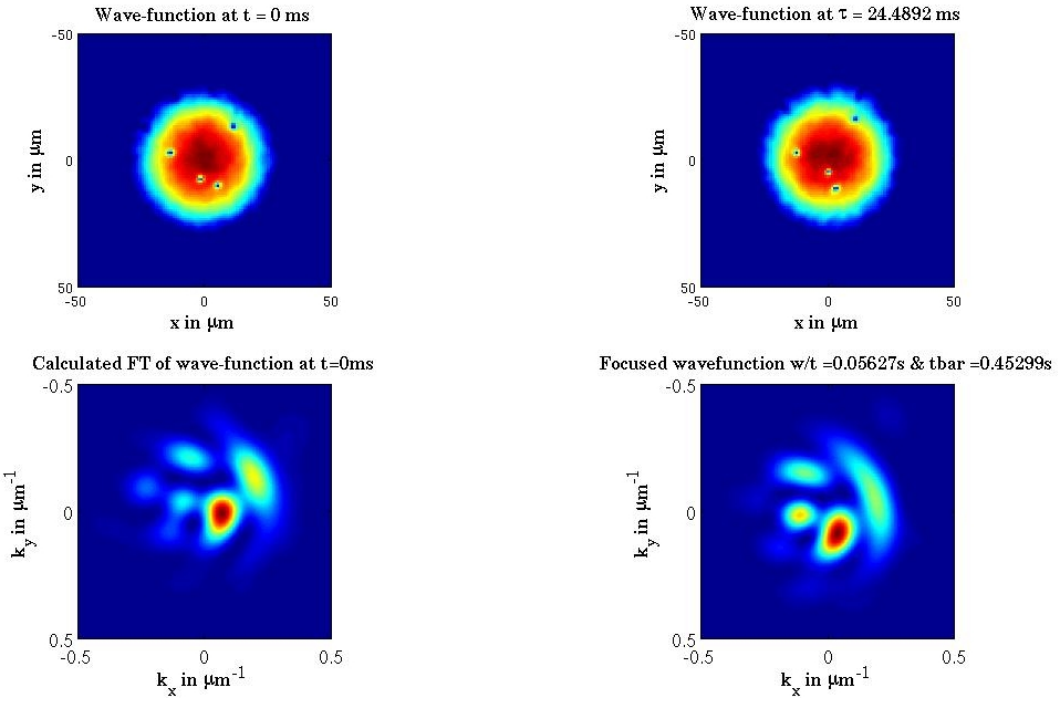


FIGURE 3.14. Fourier Transform of BEC with 4 vortices in Harmonic Trap

by a simulation of a laser beam that is stirred with different velocities through the atomic cloud. Although this procedure produces more than one pair of vortices. The final state is very unpredictable after long simulation times. On top of that, the BECs need a lot of interpretation. Looking at the graph for the state with three vortices, it might catch the attention of the reader, that, depending on the time passed in the evolution, two or three more vortices are visible at the very edge of the BEC. Their energy, however, is so small, that they do not count into the effective number of vortices. When talking about the use of the Fourier transform, we will discuss this feature further.

Second, a wide set of BEC states in a toroidal trap was on hand. After an original stirring process, where the laser beam starts at the center and is stirred with a diameter of $5.7\ \mu\mathrm{m}$ in $t = 333\ \mathrm{ms}$ through a BEC, the BEC sits in the trap for about 15 seconds. After the initial creation of vortices and a turbulent state, the number of vortices decreases slowly.

As mentioned in one of the earlier sections, the parameters we had to use to simulate

the evolution in the trap to obtain the experimental Fourier transform were slightly off. This is noticeable when comparing the state at time $t = 0\ \mathrm{ms}$ and the evolved state after $\tau$. The two states are slightly different in size. This problem occurred for different simulation methods. The simulations in this thesis are all two-dimensional simulations, which leads to a certain nonlinear term. However, depending on the assumed form of the BEC, this nonlinear parameter obtains very different values.

As discussed in section 3.3 we were not able to "translate" the nonlinear and trap parameters into the two-dimensional case, which means, that these simulations are not comparable to the real experiments. As this thesis is mainly a study of feasibility it is still interesting and educating to look at those simulations (figure 3.15 - 3.20).

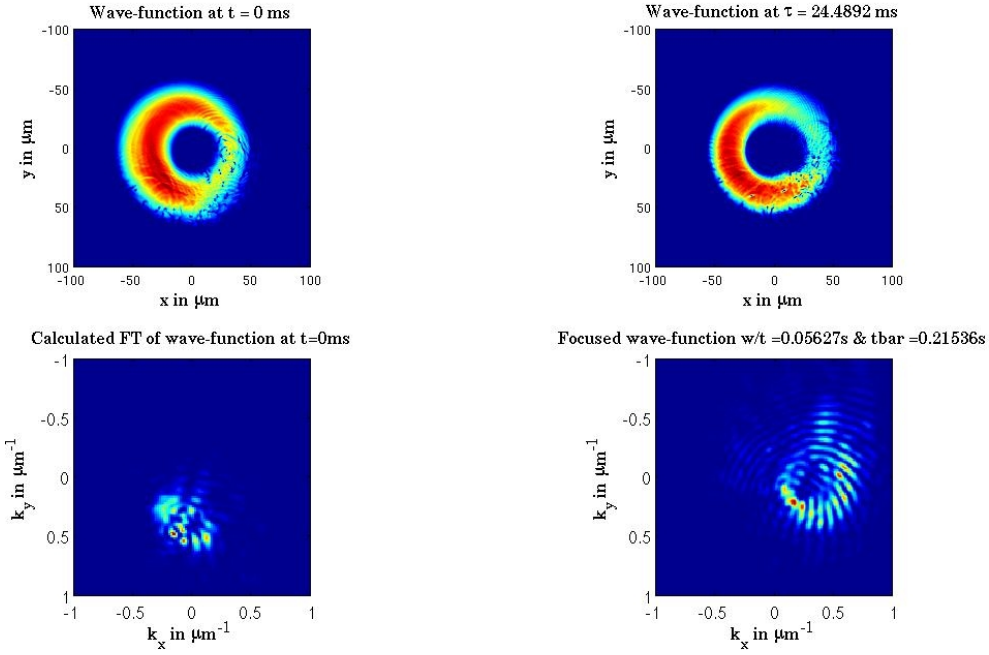


FIGURE 3.15. BEC, after propagation in trap for $t_{\mathrm{hold}} = 1\ \mathrm{ms}$

As discussed before, all the examples, independent of the form of the trap, yield certain characteristics. The Fourier transforms at $t = 0\ \mathrm{ms}$ and $\tau$ are close and seem to be similar. However, most times, one would not think, that those two are reasonable and sufficiently close. In the next chapter, when the BECs are also quantitatively analyzed,

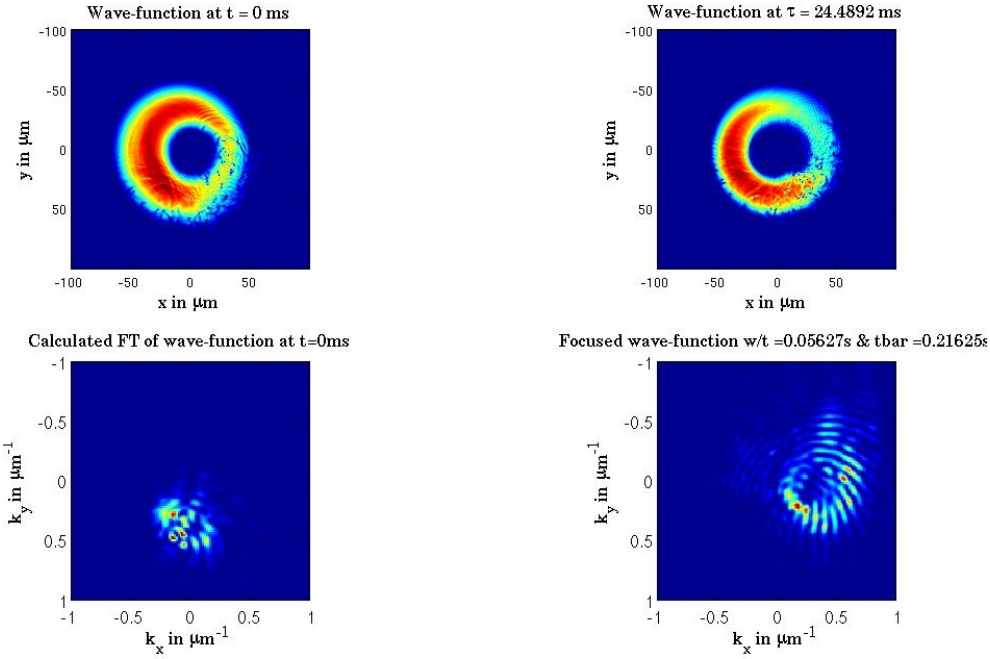


FIGURE 3.16. BEC, after propagation in trap for $t_{\text{hold}} = 51$ ms

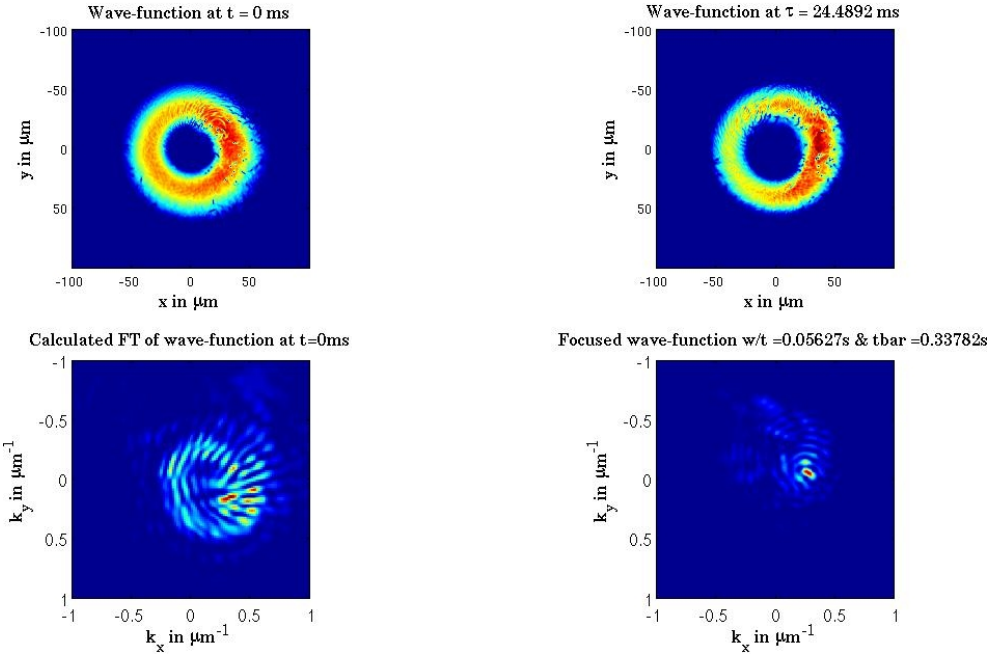


FIGURE 3.17. BEC, after propagation in trap for $t_{\text{hold}} = 5131$ ms

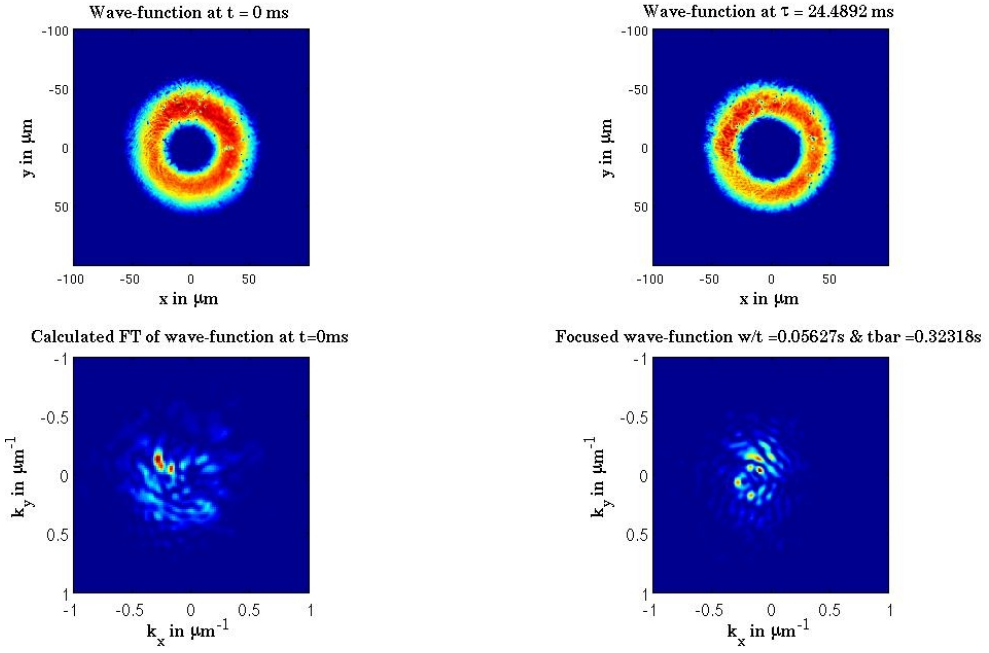


FIGURE 3.18. BEC, after propagation in trap for $t_{\mathrm{hold}} = 6158$ ms

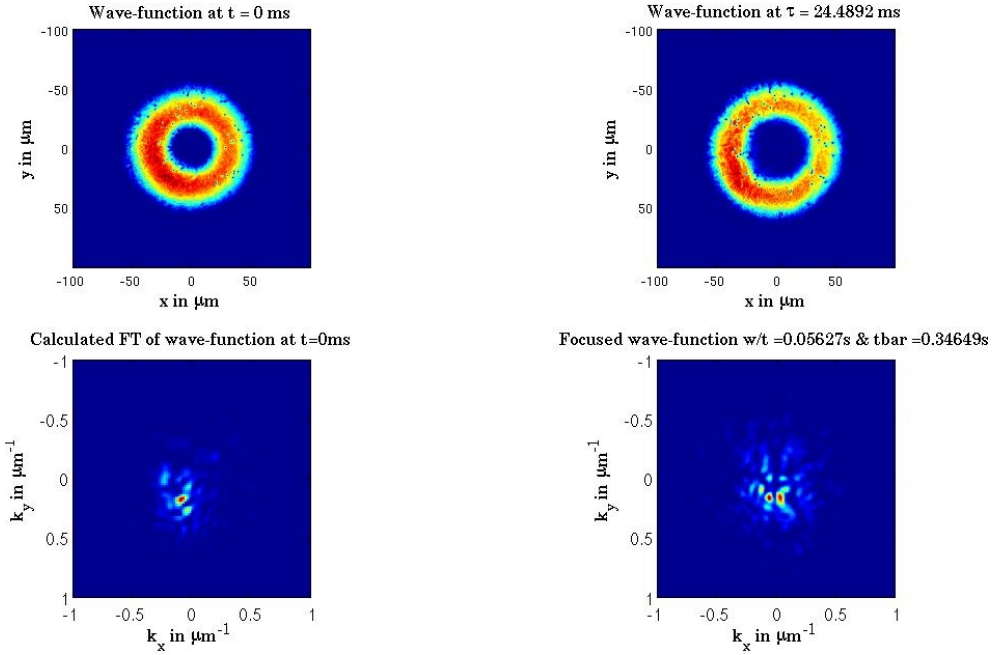


FIGURE 3.19. BEC, after propagation in trap for $t_{\mathrm{hold}} = 10262$ ms

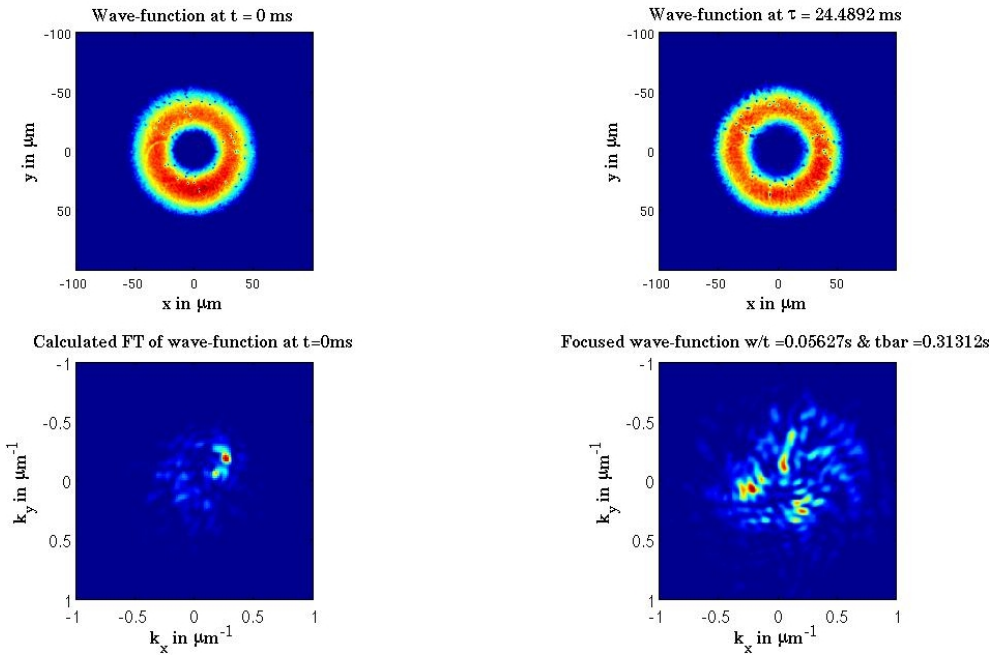


FIGURE 3.20. BEC, after propagation in trap for $t_{\mathrm{hold}} = 14362$ ms

especially concerning their coherence length, it actually shows up that those two Fourier transforms contain the same informations.

# Chapter 4

# USE OF THE DENSITY IN MOMENTUM SPACE OF A BEC

This discussion finally leads us to the quantitative analysis of a BEC and how we can make use of the obtained density in $\boldsymbol{k}$-space.

## 4.1 Coherence of a BEC

We are interested in obtaining a quantitative measure of a BEC's coherence length or off-diagonal long-range order. This value describes the phase uniformity of a BEC. The coherence length of a BEC in the ground state is at least as large as the BEC itself, since the BEC phase can be described by a constant value.

States that include vortices, or are turbulent, lead to a decreased coherence length. This allows conclusions to be drawn about the nature of a BEC and can mark a transition between turbulent and non-turbulent states.

The density matrix

$$\rho(\boldsymbol{r}, \boldsymbol{r'}) =< \hat{\psi}(\boldsymbol{r'})^{\dagger}\hat{\psi}(\boldsymbol{r}) > \tag{4.1}$$

with the creation ($\hat{\psi}^{\dagger}$) and annihilation operator ($\hat{\psi}$) is connected to the density in $\boldsymbol{k}$-space (as shown in reference [7] by

$$n(\boldsymbol{p}) = \frac{1}{V}\int \mathrm{d}\boldsymbol{R}\int \mathrm{d}\boldsymbol{s}\cdot\rho\left(\boldsymbol{R}+\frac{\boldsymbol{s}}{2}, \boldsymbol{R}-\frac{\boldsymbol{s}}{2}\right)\mathrm{e}^{-\frac{i}{\hbar}\boldsymbol{p}\cdot\boldsymbol{s}}, \tag{4.2}$$

where the authors introduced the center-of-mass coordinate $\boldsymbol{R} = \frac{\boldsymbol{r}+\boldsymbol{r'}}{2}$ and the relative coordinate $\boldsymbol{s} = \boldsymbol{r} - \boldsymbol{r'}$.

It is a common measure of coherence to look at the interference between two points of a BEC. This was achieved in 2000 by quantum optics groups in Munich [6] for a quasi one-dimensional BEC in a harmonic trap that had the form of a cigar. The approach of the

groups was, as discussed in the introduction, to excite two regions at a very well defined distance $s$ with slightly different energies and study the visibility of resulting interference fringes.

This method resembles the measurement of the spatial coherence of a light-source using a Young's double-slit. As a result, one can define visibility and coherence equivalent to optics. This was done in a review paper [12] by Naraschewski and Glauber. In this paper the authors define the degree of first-order coherence as

$$g = \frac{\rho(\boldsymbol{r}, \boldsymbol{r'})}{\sqrt{\rho(\boldsymbol{r}, \boldsymbol{r})} \cdot \sqrt{\rho(\boldsymbol{r'}, \boldsymbol{r'})}}. \tag{4.3}$$

Assuming both intensities of the laser beams are equal, the degree of coherence is equivalent to the visibility. The parameter of the visibility is very easily measurable and gave access to the coherence in the experiment with the one-dimensional BEC.

This method does not work for a two-dimensional oblate BEC. It is already complicated to pick well-defined locations for the interference of two atoms in the one-dimensional case, in the two-dimensional case this approach is experimentally impractical. However, similar to the experiment in 2000, there is a possibility to connect the Fourier transform of the density in $\boldsymbol{k}$-space to the correlation function averaged over all center-of-mass positions for a fixed relative coordinate $s$

$$\rho(s) = \int \mathrm{d}\boldsymbol{R} \cdot \rho\left(\boldsymbol{R} + \frac{\boldsymbol{s}}{2}, \boldsymbol{R} - \frac{\boldsymbol{s}}{2}\right). \tag{4.4}$$

Using equation (4.2) it is obvious that $\rho(\boldsymbol{s})$ and $n(\boldsymbol{k})$ are related by a Fourier transform. The Density Matrix[1] of the BEC state that contains four vortices looks like figure 4.1

### 4.1.1 Correlation Length

Using the Fourier transform to access the density matrix or correlation function $\rho(\boldsymbol{s})$, unfolds the way to a measure of the coherence length. Since the normalized density-matrix

[1] Plots for all states discussed in this thesis are plotted in Appendix C

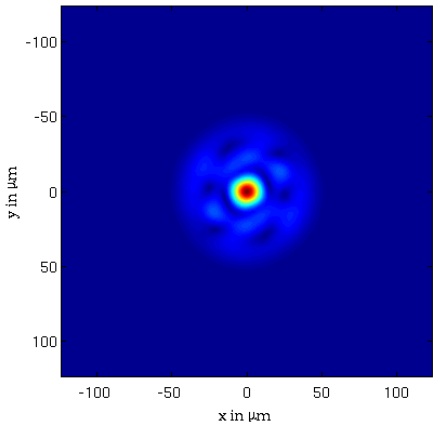


FIGURE 4.1. Density matrix of state with 4 vortices

is equivalent to the visibility, it is a valid measure of the coherence length. In a one-dimensional density matrix, one possible approach to the question on how to handle this value was to determine the full-width half-maximum (FWHM). This quantity is not that easily accessible in a two-dimensional asymmetric plot.

We decided to solve this issue in two different ways. Studying the FWHM automatically implies a loss of information, since one needs to reduce the problem to one dimension. The approach chosen in this thesis is to make 16 cuts through the two-dimensional BEC (see figure 4.2) and average over all 16 FWHM. For a reasonably smooth BEC, this results in a rather representative value for the width of the peak and therefore for the coherence length.

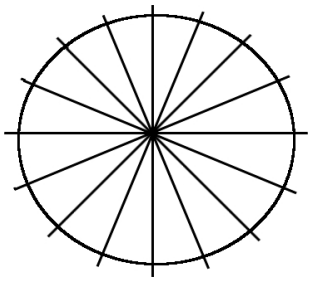

FIGURE 4.2. An illustration of eight slices used average over the FWHM.

A second approach to this problem is the RMS. With

$$< x >= \frac{\int x \cdot f(x,y)\mathrm{d}x\mathrm{d}y}{\int f(x,y)\mathrm{d}x\mathrm{d}y}$$

$$< x^2 >= \frac{\int x^2 \cdot f(x,y)\mathrm{d}x\mathrm{d}y}{\int f(x,y)\mathrm{d}x\mathrm{d}y}$$

$$\Delta_x =< x^2 > - < x >^2$$

and the same definitions for y, the RMS for the two-dimensional distribution is given by

$$\Delta = \sqrt{\Delta_x^2 + \Delta_y^2}$$

It is easily seen that the RMS gives rise to terms that are at the edge of the BEC and therefore carry less energy. Additionally we are only interested in the main peak of the density matrix and would like to blend out other information contained in the distribution. Therefore, the RMS is a very interesting quantity and worth mentioning but the ”FWHM“ is going to be the value that behaves as expected for a coherence length.

For a deeper understanding of the stability and impacts of the experiment, comparing the numerically computed Fourier transforms as well as the simulated experimental Fourier transform are the clue. These use different $\boldsymbol{k}$-spaces and for an easier implementation, it is interesting to point out the factors that are needed to transform the original real-space $\rho$ into the real-space $\rho_{\mathrm{dm}}$ in which we obtain the density matrix, so that

$$\rho_{\mathrm{dm}} = \mathrm{factor} \cdot \rho.$$

**Direct Fourier transform:** In the simulations it is necessary to increase the real-space to obtain a sufficient resolution. If $N_x$ is the original number of points in real-space and $N_{\mathrm{max}}$ is the number of points of the Fourier transform, the real-space transforms like

$$\mathrm{factor} = \frac{N_{\mathrm{max}}}{N_x} x.$$

**Simulation of Experiment:** Here, the $\boldsymbol{k}$-space is proportional to the real-space

$$dk_x = \frac{m}{\hbar t'}\lambda^2 dx,$$

where $d$ represents the spacing. Therefore,

$$\text{factor} = \frac{N_x \pi \hbar t'}{2m\lambda^2 x_{\max}^2}.$$

### 4.1.2 Results for Non-Turbulent BECs

Non-turbulent BECs, such as the BECs introduced in the beginning obtaining different numbers of vortices, are expected to have a rather large coherence length. The more vortices are introduced into the BEC, the more this quantity decreases. Earlier it was discussed that although seeing 5 vortices in one of these states, it really only is an effective 3-vortex state. This should show up in these results with a FWHM that is in the center between the BEC with only one pair and the BEC with two pairs of vortices.

Table 4.1 compares different density matrices with each other. In the simulation there is

| Number of Vortices | direct FT at $t = 0$ ms | direct FT at $\tau$ | difference [%] |
|---|---|---|---|
| 0 | 69.28 $\mu$m | 69.26 $\mu$m | 0 |
| 2 | 47.90 $\mu$m | 37.60 $\mu$m | 21.50 |
| 3 | 29.10 $\mu$m | 29.34 $\mu$m | 2.89 |
| 4 | 25.58 $\mu$m | 23.94 $\mu$m | 6.40 |

TABLE 4.1. Full-Width Half-Maximum for the density matrix of non-turbulent BECs

the possibility of directly calculating the Fourier transform of a state, which is meant by "direct Fourier transform". As always, one is also interested in the Fourier transform of the original state, and the state that is in reality Fourier-transformed, which maps to a state at a later time of the evolution in the trap.

When comparing the difference between the calculated Fourier transform and the simulations of the experiment, we concluded that the second approach needed more effort for the computation. Analyzing the values for the ground state, one expects all of the values

to be exactly the same if the damping is turned off. Therefore, since those looked exactly the same in figure 3.7, it is sufficient to only look at the numerical Fourier transform at the later time $\tau$ . The numerically calculated Fourier transforms lead to the same number for the full-width half-maximum in the ground state.

To receive a better insight to how much the evolution for time $\tau$ in the trap changes the property of the BEC, it is best to compare the differences between the values in percent of the direct Fourier transform at time $t = 0\ \mathrm{ms}$. These values decrease with more vortices are in the atom cloud. This is comprehensible, when imagining how the evolution in the trap changes the state of the BEC. A crucial detail to recall is that the density matrix calculated is averaged over all center-of-mass coordinates. The more vortices in the trap, the less change that will occur between both states when averaging over all points in the BEC.

At first glance it appears strange, that the state with only three vortices is less influenced by the propagation in the trap than the state with four vortices. Remembering, that this state had about 6 vortices, of which 3 were positioned at the edge of the BEC and therefore is only a quasi three-vortex state, gives an explanation for this phenomena. Another reason for the smaller change with more vortices is the broader distribution of the latter. Vortices that are very close to each other or rotate rather quickly around each other introduce more changes on a smaller time scale. The vortices in the state with only one pair are very close to each other and therefore one expects a bigger change in $\boldsymbol{k}$-space and therefore in the density-matrix, which leads to a different value for the full-width half-maximum. In general, we can conclude that those values meet our previous expectations and the coherence length decreases for an increasing number of vortices.

The second quantity of interest is the RMS: There are several interesting features to the RMS, however, there are theoretically no conclusions to whether this value really leads to information about the coherence length. Although the values of the full-width half-maximum and RMS for the states are pointed out in this thesis, further research is necessary to make use of this information.

| Number of Vortices | direct FT at $t = 0$ ms | direct FT at $\tau$ | difference [%] |
|---|---|---|---|
| 0 | 77.89$\mu$m | 77.86$\mu$m | -0.03 |
| 2 | 79.56 $\mu$m | 74.71 $\mu$m | -6.10 |
| 3 | 81.96 $\mu$m | 81.93 $\mu$m | -0.037 |
| 4 | 83.39 $\mu$m | 87.59 $\mu$m | -5.04 |

TABLE 4.2. RMS for the density matrix of non-turbulent BECs

The values of the RMS tend to increase for an increasing number of vortices, they behave anti proportional to the behavior of the full-width half-maximum. One reason for this feature might be, that the RMS scales with the size of the BEC and for every extra vortex that is introduced the size slightly increases. Therefore it could be a possible measure of turbulence (generally, the more vortices, the more turbulent a state is), but it seems it is rather a measure of the number of vortices in a certain trap. It also circumvents the comparison with other sizes of BECs, without additional scaling. Additionally, the observation regarding the differences of the parameters of a BEC at different times in the trap still yields that the more vortices that are observed in a BEC, the more stable the coherence length of that BEC is.

### 4.1.3 Results for the Turbulent BECs

For the atom clouds that were originally trapped in a toroidal trap, one can look at the exact same parameters.

In table 4.3 there are several interesting aspects to spot. First of all, the full-width half-maximum of a BEC in a toroidal trap is much smaller than the equivalent values for the harmonic trap. If the FWHM really depicted the coherence length and included all information, it would not be understandable why the full-width half-maximum for the ground state of the toroidal trap, which does not include any vortices, is so much smaller than the full-width half-maximum for the ground state of the harmonic trap. One possible explanation for the difference between the two of them, could be, that one averages the original

| Time after stirring process [ms] | direct FT at $t = 0$ ms | direct FT at $\tau$ | difference [%] |
|---|---|---|---|
| ground state | 11.58 $\mu$m | 11.35 $\mu$m | -1.99 |
| 1 | 19.05 $\mu$m | 11.31 $\mu$m | -40.64 |
| 51 | 19.95 $\mu$m | 11.24 $\mu$m | -43.63 |
| 1027 | 14.69 $\mu$m | 10.68 $\mu$m | -27.31 |
| 5131 | 10.84 $\mu$m | 12.77 $\mu$m | +17.84 |
| 6158 | 12.12 $\mu$m | 15.76 $\mu$m | +29.97 |
| 10262 | 16.01 $\mu$m | 13.51 $\mu$m | -15.50 |
| 14362 | 14.88 $\mu$m | 10.28 $\mu$m | -30.93 |

TABLE 4.3. Full-Width Half-Maximum for the density matrix of turbulent BECs

density matrix over all center-of-mass coordinates which returns a density matrix that depends only on the distance $\boldsymbol{s}$. Since there is zero density in the center of the toroidal trap, that is a potential reason for this result.

Another feature worth mentioning is the big discrepancy one can find between the values before the expansion and the values of the BEC after some expansion for time $\tau$ in the trap. There are several aspects that might explain this. One factor is the mismatching nonlinear parameters that were used in the simulations for this thesis and in the simulations that produced these states. This mismatch can be very well seen when propagating the toroidal groundstate for some time in the toroidal trap as seen in figure 4.3. The small mismatch in the potential introduces some sudden disturbances that can result in a small off set. The best number that gives an idea of the size of the off set is the half-width half-maximum for the ground state, which should not evolve in time and therefore be the same, even after an additional evolution in the trap. It is easily identifiable that the ground state changes over the course of the evolution: Additionally to the off set in the parameters, there is the above mentioned fact of the very fast change in the momentum-space due to close vortices. Studying the pictures of the discussed states (fig. 3.8, 3.14 - 3.19) one can see, that the better distributed the vortices are in the trap, the smaller the difference between the original state and the studied state.

An aspect worth discussing is definitely the trend of the values for the FWHM. With

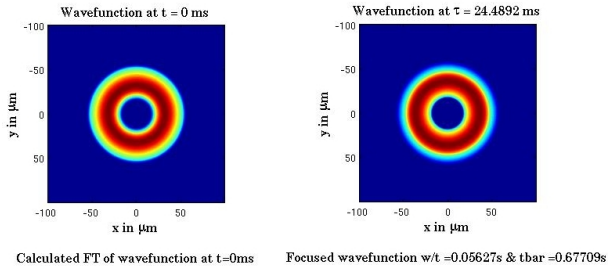


FIGURE 4.3. Time Evolution of Groundstate in Toroidal Trap

progressing $t$ for the hold in the trap after the original stir that produced the vortices, an increasing coherence length is expected, since vortices of opposite circulation start recombining. This results in a state that becomes less turbulent until it ends up back in the ground state.

In the simulations the FWHM decreases at first before it starts to increase. This decrease is owed to the vortices that start spreading all over the BEC, before they start recombining. A state that has a rather even distribution of vortices will have a smaller FWHM, since the density matrix is averaged over the whole cloud. That is also an explanation for the instability of the later increase of the FWHM, since every recombination leads to an uneven distribution. An uneven distribution favors the redistribution of vortices over the recombination which results in a decreasing FWHM. Both process would probably lead to a rather oscillating increase.

The last interesting result in the table is the increase of the FWHM comparing the ground state and the turbulent states. This result definitely needs more research; a guess could be that the averaging with more vortices leads to an accidental constructive interference due to vortices when calculating the density matrix that results in the decay of the influence of the potential well and therefore the zero density in the center.

As discussed for the non-turbulent states, the RMS is mainly a measure for the size of the original BEC. The less vortices and the less turbulent a state, the smaller a BEC and therefore the smaller the RMS. The differences between both states are between 1 and 10%,

| Time after stirring process [ms] | direct FT at $t = 0$ ms | direct FT at $\tau$ | difference [%] |
|---|---|---|---|
| ground state | 133.6 $\mu$m | 121.9 $\mu$m | 8.76 |
| 1 | 179.4 $\mu$m | 189.5 $\mu$m | 5.63 |
| 51 | 180.7 $\mu$m | 189.1 $\mu$m | 4.65 |
| 1027 | 167.6 $\mu$m | 174,2 $\mu$m | 3.94 |
| 5131 | 189.3 $\mu$m | 182.7 $\mu$m | 3.49 |
| 6158 | 166.7 $\mu$m | 189.8 $\mu$m | 13.86 |
| 10262 | 157.1 $\mu$m | 175.5 $\mu$m | 11.70 |
| 14362 | 156.1 $\mu$m | 159.0 $\mu$m | 1.86 |

TABLE 4.4. RMS for the density matrix of turbulent BECs

which is reasonable, remembering all the already mentioned issues with the simulations.

### 4.1.4 Sensitivity Study for the Coherence length

A very interesting question in the experiments is how sensitive a method is to measuring uncertainties. This was already discussed in Section 3.3, when we compared states for off set back-focusing times. Having a quantitative number one is interested in accessing through the experiment leads to the exact same question for this parameter. Therefore, figure 4.4, 4.5 and 4.7 show the percentage difference between the actual value of the FWHM [2] compared to the value obtained by applying the "wrong" back-focusing time. For the state with 2 vortices the percentage of the difference of the back focusing time $t$ from the real value $t'$ is bigger than the caused variance of the full-width half-maximum from its real value. One can therefore determine the full-width half-maximum even with a better accuracy than the other measuring parameters. For the case with three vortices, the same conclusions as for the earlier case hold. The uncertainty in $t'$, which is another way of talking about uncertainties in the pulse strength, scales at the most linear with $t'$. This is a very encouraging result. On top of that, it seems, that measuring the difference between the FWHM at one time and the FWHM at a time-step earlier, could be a way to determine

[2]The actual value in this case refers to the FWHM of the state that was produced by simulating the experiment. This has to be the case, to be able to off set the back-focusing time $t'$

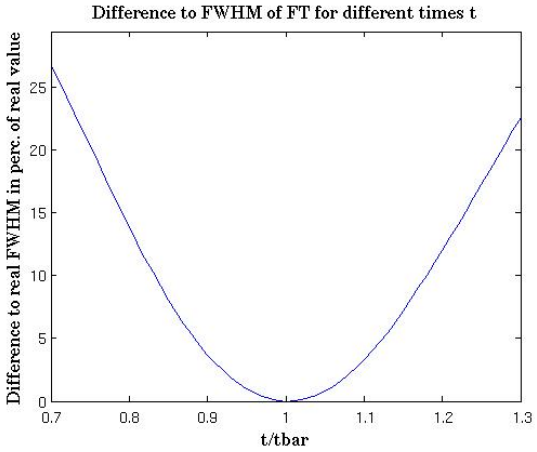


FIGURE 4.4. Study of the sensitivity of the full-width half-maximum to back-focusing times t, that differ from the true value at which the Fourier transform is obtained.
The state analyzed obtained a pair of vortices.

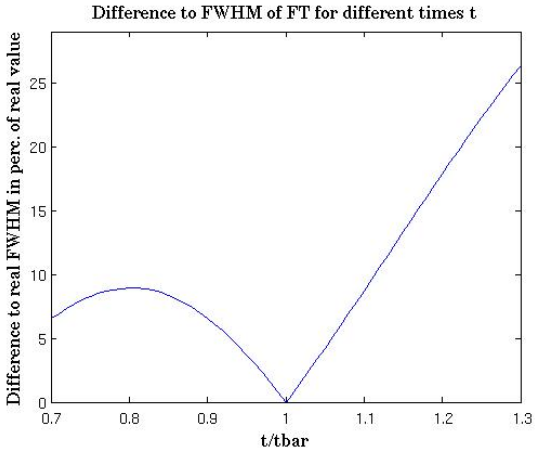


FIGURE 4.5. Study of the sensitivity of the full-width half-maximum to back-focusing times t, that differ from the true value at which the Fourier transform is obtained.
The state analyzed obtained three vortices.

the time at which one obtains the Fourier transform of the state. This leads to the plots in figure 4.6 for a state with 2 and 3 vortices. This condition seems to be almost true, although it does not hold perfectly for the case with 2 vortices.

In the turbulent case (see figure 4.7), however, this uncertainty does grow faster than the uncertainty added to $t'$. The important fact to notice is, that this behavior is even worse

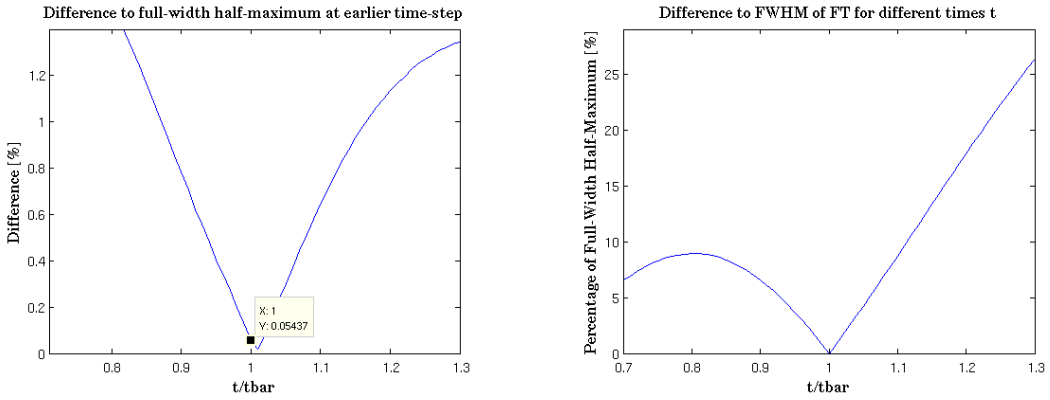


FIGURE 4.6. Calculated difference between the full-width half-maximum at time $t$ and the time step before for a state with two vortices on the left hand and three vortices on the right hand.

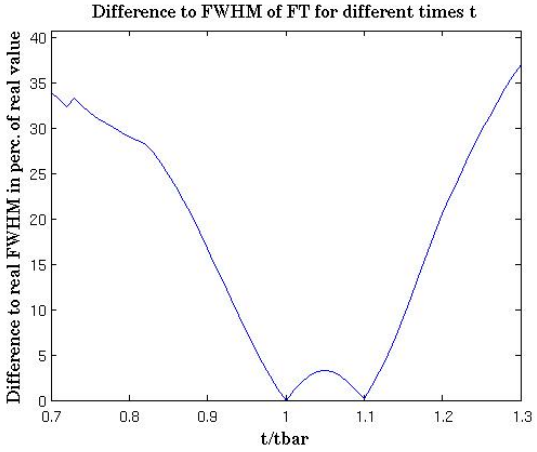


FIGURE 4.7. Study of the sensitivity of the full-width half-maximum to back-focusing times t, that differ from the true value at which the Fourier transform is obtained.
The state analyzed was originally trapped in a toroidal trap.

for smaller variations from $t'$. It is still not worse than a factor of 1.5, which is not a real obstacle, considering the very high accuracy of time and pulse strength measurement.

Importantly, one can conclude from this plot is that looking at figure 4.8, the minimum difference between a FWHM and the preceding value is not a valid measure to determine the position in time of the Fourier transform experimentally.

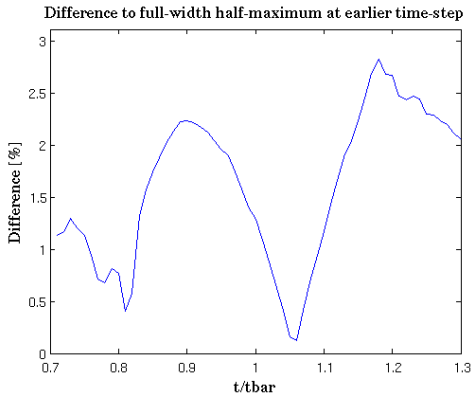


FIGURE 4.8. Variation of the back focusing time $t'$: The difference between the full-width half-maximum between two time steps is evaluated.

## 4.2 The Kinetic Energy

Another parameter one can obtain from knowing $n(\boldsymbol{k})$ is the kinetic energy, which is given by

$$E_{\text{kin}} = \frac{\hbar^2}{2m} \int_{-\infty}^{+\infty} \int_{-\infty}^{+\infty} \mathrm{d}k_x \mathrm{d}k_y k^2 \cdot |\phi(\boldsymbol{k}, t)|^2. \tag{4.5}$$

The kinetic energy is an interesting parameter, since it is not only accessible as a property of a superfluid but also measurable when working with classical fluids. One reason to do research with quantum-mechanical superfluids is the hope to be able to draw conclusions of the properties of classical liquids. For classical liquids so far only statistical properties are accessible, whereas the microscopical properties of BECs are well-known. For a comparison, however, these microscopical properties need to be translated into statistical properties, such as the kinetic energy or the coherence length.

The big difference between classical liquids and superfluids is that a BEC is a dilute gas and therefore compressible. The basic theory of classical fluids, however, usually accounts for incompressible kinetics. Therefore there is further need to develop a theory for the kinetic energy of the joint compressible and incompressible part of the kinetic energy, which is obtained from the simulations in this thesis.

The kinetic energy can be plotted in dependence of $k$, when integrating over the

phase:

$$E_{\text{kin}}(k_i + \frac{\text{dk}}{2}) = \frac{\hbar^2}{2m} \int_0^{2\pi} \int_{k_i}^{k_i+\text{dk}} \text{d}\alpha \text{d}k k^3 \cdot |\phi(k, \alpha, t)|^2,$$

where $E_{\text{kin}}$ depends on discrete values $k_i = 0, \text{dk}, ..., k_{\text{max}} - \text{dk}$ and $\boldsymbol{k} = k\text{e}^{i\alpha}$.

### 4.2.1 Kinetic Energies for Non-Turbulent BECs

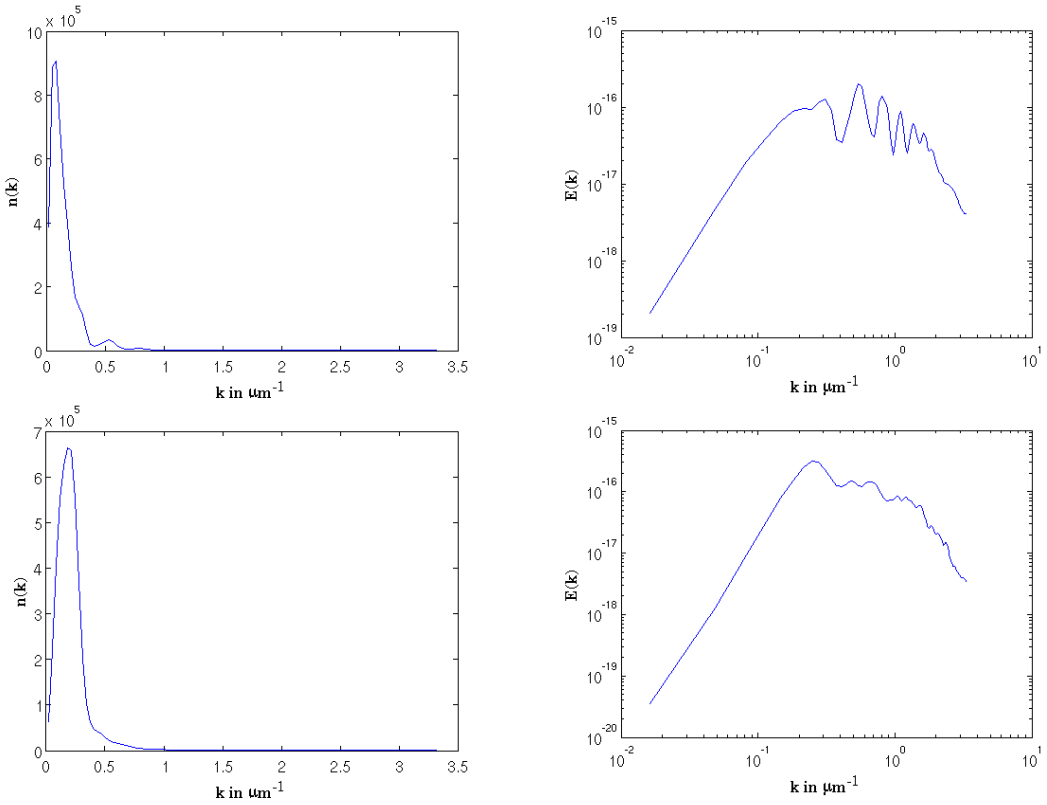


Here, the upper two graphs correspond to the kinetic energy and density distribution for the state with a single vortex dipole whereas the lower two graphs correspond to the distributions for the state with two vortex dipoles.

### 4.2.2 Kinetic Energies for Turbulent BECs

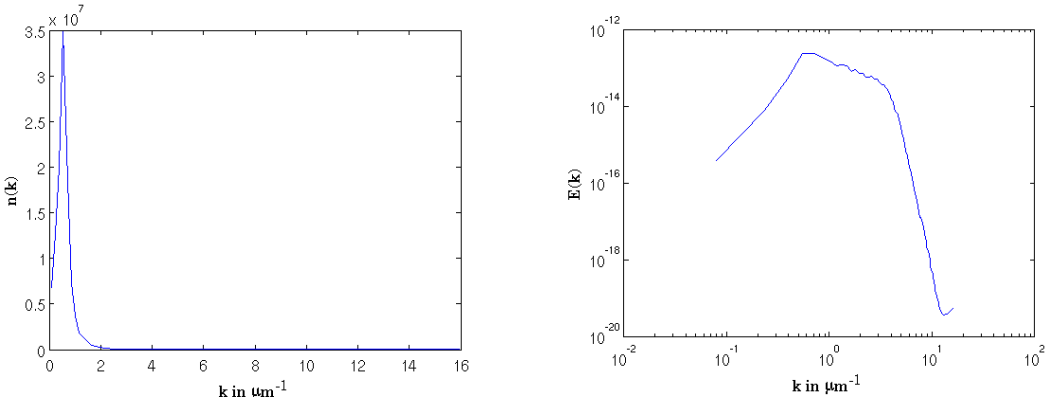


These plots were done for a BEC that was confined in the toroidal trap for another $t_{\text{hold}} = 1027\ \text{ms}$ after the creation of the vortices.

# Chapter 5
# CONCLUSIONS

Because the momentum-space distribution of a BEC can be used to obtain kinetic energy distributions or coherence lengths there is an experimental need for finding ways to obtain the momentum-space Fourier transform of a BEC. As seen in chapter 1, there have been a couple of groups successful at introducing a procedure to obtain this Fourier transformation for different lab setups, in one as well as in two dimensions. The traps used at the Bose-Einstein Condensation Lab at the University of Arizona are highly oblate but not quasi two dimensional and therefore alternatives to simple trap expansion are needed. In the thesis we discussed two different methods to obtain a Fourier transform of BECs originally in such traps, both harmonic and toroidal. Those procedures are very similar and therefore have most of the features in common.

In the thesis we were able to demonstrate numerically that an two-dimensional expansion of a highly oblate BEC which is followed by refocusing in a plane while the third dimension expands yields a Fourier transform of the initial BEC state. A minor disadvantage is that the Fourier transform obtained is a Fourier transform of a state at a later time $\tau$ in the trap: With the method introduced the initial state at time $t = 0\ \mathrm{ms}$ is experimentally not accessible. The spatial as well as the time scales are sensitive to off sets of the pulse strength which might be an issue in the application of the experiment. This holds especially, since the only way to show that a Fourier transform of the initial state was obtained is theoretical. There is no experimental accessible feature like for example a minimum size of a beam after a Fourier transform by a lens in optics.

On top of that we found a way to expand a toroidally trapped BEC in such a way, that the expanded BEC remains toroidal. This may help experimental procedures for imaging vortices in toroidal BECs.

Further areas for research can be seen. Using the momentum distribution information related to coherence lengths and kinetic energy spectra can be obtained. To interpret the relevant calculations accurately more theory has to be developed.

# Appendix A

# MATLAB CODE

## Parameters for the Simulations

```
function [ sx,sy,sz,lz,lx,ly,U0,U2,mu,Rx,Ry ] = parameters( hbar,m,wx,wy,wz,a,N )
%   returns parameters for split-step method
%   standard input values in parameters.mat
sx = sqrt(hbar/m/wx);
sy = sqrt(hbar/m/wy);
sz = sqrt(hbar/m/wz);

lz = sqrt(2*pi)*sz;
lx = sqrt(2*pi)*sx;
ly = sqrt(2*pi)*sy;

U0 = 4*pi*hbar^2*a/m;
U2 = U0/lz;

mu = sqrt(U2*(N-1)*m*wx*wy/pi);
Rx = sqrt(2*mu/m/wx^2);
Ry = sqrt(2*mu/m/wy^2);

end
```

## Defining Real- and $k$-Space

```
function [ x,y,kx,ky,dx,dy,xmax,ymax,dkx,dky,kxmax,kymax] = variables(xmax,ymax,Nmax )
%   Calculates real and k-space
%   input parameters xmax,ymax (where x,y run from -xmax/-ymax to
%   xmax/ymax
dx = 2*xmax/Nmax;
dy = 2*ymax/Nmax;

v=0:1:Nmax-1;
[x,y] = meshgrid(v,v);

x = -xmax + x*dx;
y = -ymax + y*dy;

%%%%%%%%%%%%%%%%%%%%%%%%%%%%%%%%%%
```

```
% defining k-space
%%%%%%%%%%%%%%%%%%%%%%%%%%%%%%%%%%%
c=-v+Nmax;
d=v;
e=min(c,d);

dkx=2*pi/2/xmax;
dky=2*pi/2/ymax;
kxmax=pi/dx;
kymax=pi/dy;
[kx,ky]=meshgrid(e,e);

kx=kx*kxmax/max(max(kx));
ky=ky*kymax/max(max(ky));

end
```

### Normalized Hermite Gaussians[1]

```
function [ H ] = HG( n,x,a )
%returns a normalized hermite gaussian
%  n: order of the hermite gaussian polynomial
%  x: position variable
%  a: harmonic oscillator length = sigma/sqrt(2)

coef = HPcoef(n);

HP = 0;

for p=n:-2:0
    HP = HP + coef(p+1)*(x/a).^p;
end

H = HP .* exp(-(x/sqrt(2)/a).^2);

dx = abs(x(2)-x(1));

norm = dx*sum(sum(H.*H));

H=H/sqrt(norm);

end
```

### Calculating the Coefficients for the Hermite Polynomials[2]

[1] Code written by Z.Newman and B.P.Anderson
[2] Code written by Z.Newman and B.P.Anderson

```
function [ coef ] = HPcoef( nmax )
%This function returns the coefficients for the hermite polynomial H_{nmax}
%   coef(1)*x^0+coef(2)*x^1+...

c = zeros(nmax+1,nmax);
c(1,1)=1;
c(2,2)=2;

for i=2:nmax
    nindex = i+1;
    c(nindex,nindex) = 2^i;
    c(nindex,1) = -2*(i-1)*c(nindex-2,1);
    c(nindex,2) = -2*i*c(nindex-2,2);
    for j=2:i-2;
        jindex = j+1;
        c(nindex,jindex) = 2*c(nindex-1,jindex-1)-jindex*...
            c(nindex-1,jindex+1);
    end
end

coef = c(nmax+1,:);

end
```

### Decomposition of a Wavefunction into Hermite Polynomials

```
function [ITN] = decomp(X, Y, Rx, Ry, sx, sy )
%this function returns ground state of BEC
%   x,y: 2D-grid
%   R: Radius of Thomas-Fermi-approximation
%   s: harmonic oscillator length

x = X(1,:);
y = Y(:,1);
%recalculate properties of x,y
dx=abs(x(2)-x(1));
dy=abs(y(2)-y(1));

%calculate Thomas-Fermi solution
phi=sqrt(2/pi/Rx/Ry)*sqrt(max(0,(1-(X/Rx).^2-(Y/Ry).^2)));

nmax=60;

% calculating coeff for decomp of phi into HG
% using fine grid, maximal HPcoef up to nmax

c = zeros(nmax+1);

```

```
for n=0:nmax
    for m=0:nmax
        if(n+m<nmax)
            Fx=HG(n,x,sx);
            Fy=HG(m,y,sy);
            F=Fy*Fx;
            c(n+1,m+1) = dx*dy*sum(sum(phi.*F));
        else
            c(n+1,m+1) = 0;
        end
    end
end


% using coef calculated above, calculating psi for "real" grid

ITN = 0;

for n = 0:nmax
    for m=0:nmax
        if (n+m < nmax)
            Fx=HG(n,x,sx);
            Fy=HG(m,y,sy);
            F=Fy*Fx;
            ITN = ITN + c(n+1,m+1) * F;
        end
    end
end

[sc sr]=size(ITN);
nx=linspace(-sc/2,sc/2,sc);
ny=linspace(-sr/2,sr/2,sr);

[KX KY] = meshgrid(nx,ny);
Yfmask=sr/4;
Xfmask=sc/4;

Fmask = exp(-KX.^2/Xfmask.^2).*exp(-KY.^2/Yfmask^2);

ITN = ifft2(Fmask.*fftshift(fft2(ITN)));
norm=dx*dy*sum(sum(abs(ITN).^2));

ITN = ITN/sqrt(norm);

plot(y,abs(phi(129,:)),y,abs(ITN(129,:)));
end
```

**Choosing $\Delta t$**

```
function [ dt ] = calculate_dt( m,wx,wy,wz,hbar,a,psi,x,kx,V,N,fac)
%CALCULATE_DT This function calculates the limits for dt
%   Detailed explanation goes here

[ ~,~,~,~,~,~,~,U2,~,~,~ ] = parameters( hbar,m,wx,wy,wz,a,N );

n = abs(psi).^2;

kmax = max(max(kx));
W = V + n.*U2*(N-1);
Wmax = max(max(W));

kappa = m/hbar/kmax^2;
chi = hbar/Wmax;

if kappa<chi
    dt=kappa*fac;
    else
    dt=chi*fac;
end

end
```

### Split-Step Method

```
function [ psi ] = split_step(psi,Nt,dt,Km,V,N,U2,eps,hbar,dx,dy)
%SPLIT_STEP function to calculate the split-step function
%   Detailed explanation goes here

for j=1:Nt

    n=(abs(psi)).^2;        %calculating first density
    W = V + n.*U2*(N-1);
    Wm=exp(-(1i+eps).*dt/2*W/hbar);

    psi=ifft2(Km.*fft2(Wm.*psi));

    n=(abs(psi)).^2;        %calculating scnd density
    W = V + n.*U2*(N-1);
    Wm=exp(-(1i+eps)*dt/2.*W/hbar);

    psi=Wm.*psi;

    norm=dx*dy*sum(sum(abs(psi).^2));   %normalization of wave-↩
        function
    psi=1/sqrt(norm)*psi;

end

```

```
24 end
```

### The Ground State

```
1  close all
2  clear all
3  clc
4
5  %%%%%%%%%%%%%%%%%%%%%%%%%%%%%%%%%%
6  % define necessary parameters
7  %%%%%%%%%%%%%%%%%%%%%%%%%%%%%%%%%%
8  load parameters.mat
9  N = 100000;
10 [ sx,sy,sz,lz,lx,ly,U0,U2,mu,Rx,Ry ] = parameters( hbar,m,wx,wy,wz,a,N↩
       );
11
12
13 %%%%%%%%%%%%%%%%%%%%%%%%%%%%%%%%%%
14 % defining x,y,kx,ky
15 %%%%%%%%%%%%%%%%%%%%%%%%%%%%%%%%%%
16 xmax = 120;
17 ymax = 120;
18 Nmax = 256;
19 [ x,y,kx,ky,dx,dy,xmax,ymax,dkx,dky,kxmax,kymax] = variables( xmax,↩
      ymax,Nmax );
20
21 %%%%%%%%%%%%%%%%%%%%%%%%%%%%%%%%%%
22 % defining V
23 %%%%%%%%%%%%%%%%%%%%%%%%%%%%%%%%%%
24 V=1/2*m*(wx^2*x.^2+wy^2*y.^2);
25
26 %%%%%%%%%%%%%%%%%%%%%%%%%%%%%%%%%%
27 % calculating ground state
28 %%%%%%%%%%%%%%%%%%%%%%%%%%%%%%%%%%
29 Rxexp=25;
30 Ryexp=25;
31 psi=decomp(x,y,Rx,Ry,lx,ly);
32 psi0ar=psi(Nmax/2+1,:);
33 psi=abs(psi);
34
35 %%%%%%%%%%%%%%%%%%%%%%%%%%%%%%%%%%
36 % defining dt
37 %%%%%%%%%%%%%%%%%%%%%%%%%%%%%%%%%%
38 tmax = 0.4;
39 dt = calculate_dt(m,wx,wy,wz,hbar,a,psi,x,kx,V,N,.1);
40 Nt = round(tmax/dt);
41
42
43 %%%%%%%%%%%%%%%%%%%%%%%%%%%%%%%%%%
```

```
% defining propagation matrix
%%%%%%%%%%%%%%%%%%%%%%%%%%%%%%%%%%%
Km=exp(-(1i+eps)*dt/m*hbar*(kx.^2+ky.^2)/2);

psi = split_step(psi,Nt,dt,Km,V,N,U2,eps,hbar,dx,dy);

%%%%%%%%%%%%%%%%%%%%%%%%%%%%%%%%%%%%%%%%%%%%%%%%%%%
%plot three states after simulation
%%%%%%%%%%%%%%%%%%%%%%%%%%%%%%%%%%%%%%%%%%%%%%%%%%%
phi=sqrt(2/pi/Rxexp/Rxexp)*sqrt(max(0,(1-(x/Rxexp).^2-(y/Ryexp).^2)));%TF solution

figure(1)
plot(yar,abs(phi(Nmax/2+1,:)).^2,yar,abs(psi0ar).^2,yar,abs(psiar).^2);
set(gca,'FontSize',15);
xlabel('y');
ylabel('|\psi|');
title('Ground - State |\psi (x,y)|');
legend('Thomas-Fermi-Solution','Decomposition of TF-solution','Groundstate');

save groundstate_N=100000.mat psi x y dt phi N
```

### Turning on a Laser Beam

```
close all
clear all
clc
load groundstate_N=100000.mat
%%%%%%%%%%%%%%%%%%%%%%%%%%%%%%%%%%%
% definition of parameters
% everything in microns
%%%%%%%%%%%%%%%%%%%%%%%%%%%%%%%%%%%
xmax = max(max(abs(x)));
ymax = max(max(abs(y)));
[Nmax,~] = size(x);
eps=0.005;
psi0 = psi;

%%%%%%%%%%%%%%%%%%%%%%%%%%%%%%%%%%%
%Harmonic Oscillator Properties
%%%%%%%%%%%%%%%%%%%%%%%%%%%%%%%%%%%
load parameters.mat
N = 100000;
[ sx,sy,sz,lz,lx,ly,U0,U2,mu,Rx,Ry ] = parameters( hbar,m,wx,wy,wz,a,N);

%%%%%%%%%%%%%%%%%%%%%%%%%%%%%%%%%%%
```

```
% defining x,y,kx,ky
%%%%%%%%%%%%%%%%%%%%%%%%%%%%%%%%%%%
[ x,y,kx,ky,dx,dy,xmax,ymax,dkx,dky,kxmax,kymax] = variables( xmax,ymax,Nmax );

%%%%%%%%%%%%%%%%%%%%%%%%%%%%%%%%%%%
% defining V
%%%%%%%%%%%%%%%%%%%%%%%%%%%%%%%%%%%
V=1/2*m*(wx^2*x.^2+wy^2*y.^2);


%%%%%%%%%%%%%%%%%%%%%%%%%%%%%%%%%%%
%defining gaussian laser potential
%%%%%%%%%%%%%%%%%%%%%%%%%%%%%%%%%%%
mu0 = 8*hbar*wz;
RL = 5;
UL = mu0;
x0 = -8;
y0 = 0;

%%%%%%%%%%%%%%%%%%%%%%%%%%%%%%%%%%%
% defining dt
%%%%%%%%%%%%%%%%%%%%%%%%%%%%%%%%%%%
tmax = .1;
dt = calculate_dt(m,wx,wy,wz,hbar,a,psi,x,kx,V,N,.1);
Nt = round(tmax/dt);
delta = 1/Nt/dt;

%%%%%%%%%%%%%%%%%%%%%%%%%%%%%%%%%%%
% defining propagation matrix
%%%%%%%%%%%%%%%%%%%%%%%%%%%%%%%%%%%
Km=exp(-(1i+eps)*dt/m*hbar*(kx.^2+ky.^2)/2);

for j=1:Nt

    t=j*dt;
    n=(abs(psi)).^2;        %calculating first density
    W = V + n.*U2*(N-1) + t*delta*UL*exp(-((x-x0).^2+(y-y0).^2)/RL^2);
    Wm=exp(-(1i+eps).*dt/2*W/hbar);

    psi=ifft2(Km.*fft2(Wm.*psi));

    n=(abs(psi)).^2;        %calculating scnd density
    W = V + n.*U2*(N-1) + t*delta*UL*exp(-((x-x0).^2+(y-y0).^2)/RL^2);
    Wm=exp(-(1i+eps)*dt/2.*W/hbar);

    psi=Wm.*psi;

    norm=dx*dy*sum(sum(abs(psi).^2));   %normalization of wave-
```

```
        function
71      psi=1/sqrt(norm)*psi;
72  end
73
74  save turn_on_beam_N=100000.mat psi x y dt N;
```

### Producing a State with two Pairs of Vortices

```
1   close all
2   clear all
3   clc
4   load turn_on_beam_N=100000.mat
5   %%%%%%%%%%%%%%%%%%%%%%%%%%%%%%%%%%
6   % definition of parameters
7   % everything in microns
8   %%%%%%%%%%%%%%%%%%%%%%%%%%%%%%%%%%
9   xmax = max(max(abs(x)));
10  ymax = max(max(abs(y)));
11  [Nmax,~] = size(x);
12  eps = 0.005;
13  psi0 = psi;
14
15  %%%%%%%%%%%%%%%%%%%%%%%%%%%%%%%%%%
16  %Harmonic Oscillator Properties
17  %%%%%%%%%%%%%%%%%%%%%%%%%%%%%%%%%%
18  load parameters.mat
19  N = 100000;
20  [ sx,sy,sz,lz,lx,ly,U0,U2,mu,Rx,Ry ] = parameters( hbar,m,wx,wy,wz,a,N↩
        );
21
22  %%%%%%%%%%%%%%%%%%%%%%%%%%%%%%%%%%
23  %defining gaussian laser potential
24  %%%%%%%%%%%%%%%%%%%%%%%%%%%%%%%%%%
25  mu0 = 8*hbar*wz;
26  RL = 5;
27  UL = mu0;
28  x0 = 8;
29  y0 = 0;
30  v0 = 300;
31  %deltax = 12;
32
33  %%%%%%%%%%%%%%%%%%%%%%%%%%%%%%%%%%
34  % defining x,y,kx,ky
35  %%%%%%%%%%%%%%%%%%%%%%%%%%%%%%%%%%
36  [ x,y,kx,ky,dx,dy,xmax,ymax,dkx,dky,kxmax,kymax] = variables( xmax,↩
        ymax,Nmax );
37
38  %%%%%%%%%%%%%%%%%%%%%%%%%%%%%%%%%%
39  % defining V
```

```
40 %%%%%%%%%%%%%%%%%%%%%%%%%%%%%%%%%%%%
41 V=1/2*m*(wx^2*x.^2+wy^2*y.^2);
42
43 %%%%%%%%%%%%%%%%%%%%%%%%%%%%%%%%%%%%
44 % defining propagation matrix
45 %%%%%%%%%%%%%%%%%%%%%%%%%%%%%%%%%%%%
46 Km=exp(-(1i+eps)*dt/m*hbar*(kx.^2+ky.^2)/2);
47
48 %%%%%%%%%%%%%%%%%%%%%%%%%%%%%%%%%%%%
49 % defining dt
50 %%%%%%%%%%%%%%%%%%%%%%%%%%%%%%%%%%%%
51 omega = v0/x0;
52 tmax = 2*pi/omega;
53 dt = calculate_dt(m,wx,wy,wz,hbar,a,psi,x,kx,V,N,.1);
54 Nt = round(tmax/dt);
55 delta = 1/Nt/dt;
56 t = 0;
57
58 for j=1:Nt
59
60     t=j*dt;
61     x1 = cos(omega*t+pi)*x0;
62     y1 = sin(omega*t+pi)*x0;
63
64     n=(abs(psi)).^2;         %calculating first density
65     W = V + n.*U2*(N-1) + (1-t*delta)*UL*exp(-((x-x1).^2+(y-y1).^2)/RL↩
           ^2);
66     Wm=exp(-(1i+eps).*dt/2*W/hbar);
67
68     psi=ifft2(Km.*fft2(Wm.*psi));
69
70     n=(abs(psi)).^2;         %calculating scnd density
71     W = V + n.*U2*(N-1) + (1-t*delta)*UL*exp(-((x-x1).^2+(y-y1).^2)/RL↩
           ^2);
72     Wm=exp(-(1i+eps)*dt/2.*W/hbar);
73
74     psi=Wm.*psi;
75
76     norm=dx*dy*sum(sum(abs(psi).^2));   %normalization of wave-↩
           function
77     psi=1/sqrt(norm)*psi;
78 end
79
80 save vortices_3_N=100000.mat psi x y dt N;
```

The code above produces the state used in the simulation with two pair of vortices. To produce the state with only one pair of vortices the beam needs to be swept linearly as

described in the thesis.

**Fourier transform**

```
close all
clear all
clc

load parameters.mat
load toroidal/stir_and_hold/BC_spiralin_smalldx_groundstate_1.mat

[ sx,sy,sz,lz,lx,ly,U0,U2,mu,Rx,Ry ] = parameters( hbar,m,wx,wy,wz,a,N↩
    );

%fac = .28;
Norm = abs(x(2,2)-x(1,1))*abs(y(2,2)-y(1,1))*sum(sum(abs(e).^2))*(fac)↩
    ^2;
psi = e/sqrt(Norm);
e = psi;

psifft = fftshift(fft2(psi,256*8,256*8));
lambda = 3;
t = sqrt(lambda^2-1)/wx;

%%%%%%%%%%%%%%%%%%%%%%%%%%%%%%%%%%%%%%%%%%%%%%%%%%%%%%%%%%%%%%%%%%%%%%%
% definition of parameters
% healing length .28 microns
% everything in microns, originally in units of healing length
%%%%%%%%%%%%%%%%%%%%%%%%%%%%%%%%%%%%%%%%%%%%%%%%%%%%%%%%%%%%%%%%%%%%%%%
xmax = max(max(abs(x)))*fac;
ymax = max(max(abs(y)))*fac;
[~,Nmax] = size(x);

%%%%%%%%%%%%%%%%%%%%%%%%%%%%%%%%%%
% defining variables
%%%%%%%%%%%%%%%%%%%%%%%%%%%%%%%%%%
[ x,y,kx,ky,dx,dy,xmax,ymax,dkx,dky,kxmax,kymax] = variables(xmax,ymax↩
    ,Nmax);
[ xhat,yhat,kxhat,kyhat,dxhat,dyhat,xmaxhat,ymaxhat,dkxhat,dkyhat,↩
    kxmaxhat,kymaxhat] = variables(xmax*lambda,ymax*lambda,Nmax);
[ ~,~,kxbig,kybig,~,~,~,~,dkxbig,dkybig,kxmaxbig,kymaxbig] = variables↩
    (xmax*8*256/Nmax,ymax*8*256/Nmax,256*8);

kr = 0;

kxmed = fftshift(kxbig);
kymed = fftshift(kybig);

kxar = zeros(256*8,1);
```

```
kyar = zeros(256*8,1);

for j = 1:(256*8)/2
    kxar(j) = -kxmed(1,j);
    kyar(j) = -kymed(j,1);
end

for j = 256*4+1:256*8
    kxar(j) = kxmed(1,j);
    kyar(j) = kymed(j,1);
end


%%%%%%%%%%%%%%%%%%%%%%%%%%%%%%%%%%
% defining V
%%%%%%%%%%%%%%%%%%%%%%%%%%%%%%%%%%
mu0 = 8*hbar*wz;
B0 = 2.2*mu;          %Choice depending on input state
w0 = .28*102;         %Choice depending on input state
V=1/2*m*(wx^2*x.^2+wy^2*y.^2) + B0*exp(-(x.^2+y.^2)/w0^2);

%%%%%%%%%%%%%%%%%%%%%%%%%%%%%%%%%%%%
% defining dt
%%%%%%%%%%%%%%%%%%%%%%%%%%%%%%%%%%%%
[dt] = calculate_dt(m,wx,wy,wz,hbar,a,psi,x,kx,V,N,1);

tmax = atan(wx*t)/wx;
Nt = round((tmax)/dt);
delta = 1/Nt/dt;

%%%%%%%%%%%%%%%%%%%%%%%%%%%%%%%%%%
% defining propagation matrix
%%%%%%%%%%%%%%%%%%%%%%%%%%%%%%%%%%
Km=exp(-(1i+eps)*dt/m*hbar*(kx.^2+ky.^2)/2);

psi = split_step(psi,Nt,dt,Km,V,N,U2,0,hbar,dx,dy);

psilab = 1/lambda*psi;
psiffttau = fftshift(fft2(psi,256*8,256*8));

%%%%%%%%%%%%%%%%%%%%%%%%%%%%%%%%%%%%%%%%%%%%%%%%%%%%%%%%%%%%
% scale the magnetic pulse
%%%%%%%%%%%%%%%%%%%%%%%%%%%%%%%%%%%%%%%%%%%%%%%%%%%%%%%%%%%%

MAX = max(max(abs(psiffttau)));


for j = 1:256*8
    for k = 1:256*8
```

```
90          if abs(psiffttau(j,k))>MAX*.005
91              if (kxmed(j,k)^2+kymed(j,k)^2)>kr^2
92                  kr = sqrt(kxmed(j,k)^2+kymed(j,k)^2);
93              end
94          end
95      end
96  end
97
98  scaling = kr/xmax;
99
100 fac = lambda^2/scaling;
101
102 %%%%%%%%%%%%%%%%%%%%%%%%%%%%%%%%%%%%%%%%%%%%%%%%%%%%%%%%%%%%
103 % apply the magnetic pulse
104 %%%%%%%%%%%%%%%%%%%%%%%%%%%%%%%%%%%%%%%%%%%%%%%%%%%%%%%%%%%%
105
106 tbar = m/hbar*fac;
107
108 eta = m/2/hbar*1/tbar;
109
110 MP = exp(-1i*eta*(xhat.^2+yhat.^2));
111
112 psibar = MP.*psilab;
113
114 %%%%%%%%%%%%%%%%%%%%%%%%%%%%%%%%%%%%%%%%%%%%%%%%%%%%%%%%%%%%
115 % let it propagate for t'
116 % use only FT, since at the point, where they apply
117 % a magnetic pulse, one releases the 3D confinement
118 %
119 % -> no interaction in density regime
120 %%%%%%%%%%%%%%%%%%%%%%%%%%%%%%%%%%%%%%%%%%%%%%%%%%%%%%%%%%%%
121
122 Km=exp(-(1i)*tbar/m*hbar*(kxhat.^2+kyhat.^2)/2);
123
124 psibar = ifft2(Km.*fft2(psibar));
125
126 psibar = psibar*2*pi*hbar*tbar/m/lambda/(dx)^2;
127
128 kxprime = m/hbar/tbar*lambda*xhat(1,:);
129 kyprime = m/hbar/tbar*lambda*yhat(:,1);
130
131 figure(3)
132 subplot(2,2,1)
133 imagesc(x(1,:),y(:,1),abs(e).^2)
134 title('Wavefunction at t = 0 ms','FontName','New Century Schoolbook','↩
      FontSize',14)
135 xlabel('x in \mum','FontName','New Century Schoolbook','FontSize',14)
136 ylabel('y in \mum','FontName','New Century Schoolbook','FontSize',14)
137 axis image
```

```
138 subplot(2,2,2)
139 imagesc(x(1,:),y(:,1),abs(psi).^2)
140 title(['Wavefunction at \tau = ',num2str(tmax*1000),' ms'],'FontName',↩
        'New Century Schoolbook','FontSize',14)
141 xlabel('x in \mum','FontName','New Century Schoolbook','FontSize',14)
142 ylabel('y in \mum','FontName','New Century Schoolbook','FontSize',14)
143 axis image
144 subplot(2,2,3)
145 imagesc(kxar,kyar,abs(psifft).^2)
146 set(gca,'FontSize',14);
147 axis image
148 axis([-kr,kr,-kr,kr])
149 title('Calculated FT of wavefunction at t=0ms','FontName','New Century↩
        Schoolbook','FontSize',14)
150 xlabel('k_x in \mum^{-1}','FontName','New Century Schoolbook','↩
        FontSize',14)
151 ylabel('k_y in \mum^{-1}','FontName','New Century Schoolbook','↩
        FontSize',14)
152 subplot(2,2,4)
153 imagesc(kxprime, kyprime, abs(psibar).^2)
154 set(gca,'FontSize',14);
155 title(['Focused wavefunction w/t =',num2str(t),'s & tbar =',num2str(↩
        tbar),'s'],'FontName','New Century Schoolbook','FontSize',14)
156 xlabel('k_x in \mum^{-1}','FontName','New Century Schoolbook','↩
        FontSize',14)
157 ylabel('k_y in \mum^{-1}','FontName','New Century Schoolbook','↩
        FontSize',14)
158 axis image
159 axis([-kr,kr,-kr,kr])
160
161 save toroidal/stir_and_hold/prop_groundstate_l=3.mat kxar kyar kxprime↩
        kyprime psibar psiffttau psifft tmax tbar N
162 save toroidal/stir_and_hold/FT_groundstate_l=3.mat x y psi t tmax tbar↩
        xhat yhat N
163 saveas(gcf,'toroidal/stir_and_hold/groundstate.fig')
```

### Full-Width Half-Maximum

```
1  close all
2  clear all
3  clc
4
5  load parameters.mat
6  load toroidal/stir_and_hold/prop_holdintrap_1_l=3.mat
7  load toroidal/stir_and_hold/FT_holdintrap_1_l=3.mat
8  %load vortices/prop_vortices_l=3.mat
9  %load vortices/FT_vortices_l=3.mat
10
11 %%%%%%%%%%%%%%%%%%%%%%%%%%%%%%%%%%%%%%%%%%%%%%%%%%%%%%%%%%%%%%%%%%%%%%%%%%%%
```

```
% calculating the radius of the BEC
%%%%%%%%%%%%%%%%%%%%%%%%%%%%%%%%%%%%%%%%%%%%%%%%%%%%%%%%%%%%%%%%%%%%%%%%%%%%
psibar = psifft;
lambda = 3;
[Nmax,~] = size (psibar);
[Nx,~] = size(x);

%Choice of factor, depending on choice of psibar
%upper factor for psibar = psibar, lower factor for numerical FT

%factor = Nmax*pi*hbar*tbar/2/m/lambda^2/max(max(abs(x)))^2;
factor = Nmax/Nx;

%%%%%%%%%%%%%%%%%%%%%%%%%%%%%%%%%%%%%%%%%%%%%%%%%%%%%%%%%%%%%%%%%%%%%%%%%%%%
% calculating n,rho,new sized grid
%%%%%%%%%%%%%%%%%%%%%%%%%%%%%%%%%%%%%%%%%%%%%%%%%%%%%%%%%%%%%%%%%%%%%%%%%%%%

n = abs(psibar).^2;
rho = fftshift(fft2(n,256*8,256*8));
[xhatbig,yhatbig,~,~,~,~,~,~,~,~,kxmax,~] = variables(max(max(abs(x)))↩
    *factor,max(max(abs(y)))*factor,256*8);
fac = 2048/Nmax;

%%%%%%%%%%%%%%%%%%%%%%%%%%%%%%%%%%%%%%%%%%%%%%%%%%%%%%%%%%%%%%%%%%%%%%%%%%%%
% cuts through BEC
%%%%%%%%%%%%%%%%%%%%%%%%%%%%%%%%%%%%%%%%%%%%%%%%%%%%%%%%%%%%%%%%%%%%%%%%%%%%
[theta,r] = cart2pol(xhatbig,yhatbig);

% going through angles at edge
width = zeros(16,1);
for j = 1:8
    [rplus,cplus] = find(theta>theta(Nmax*fac/2-3,Nmax*fac/2-3+j)-.001↩
        & theta<theta(Nmax*fac/2-3,Nmax*fac/2-3+j)+.001);
    kplus = length(rplus);
    [rminus,cminus] = find(theta>theta(Nmax*fac/2-3,Nmax*fac/2-3+j)↩
       -.001+pi & theta<theta(Nmax*fac/2-3,Nmax*fac/2-3+j)+.001+pi);
    kminus = length(rminus);

    absrhoar = zeros(kminus+kplus+1,1);
    zar = zeros(kminus+kplus+1,1);

    for q = 1:kminus
        zar(q) = -r(rminus(q),cminus(q));
        absrhoar(q) = abs(rho(rminus(q),cminus(q)));
    end

    zar(kminus+1) = r(Nmax*fac/2+1,Nmax*fac/2+1);
    absrhoar(q+1) = abs(rho(Nmax*fac/2+1,Nmax*fac/2+1));

```

```
58      for q = 1:kplus
59          zar(q+1+kminus) = r(rplus(q),cplus(q));
60          absrhoar(q+1+kminus) = abs(rho(rplus(q),cplus(q)));
61      end
62
63      [zar,sortindex] = sort(zar);
64      absrhoar = absrhoar(sortindex);
65
66      width(j) = fwhm(zar,absrhoar);
67  end
68
69  for j = 1:8
70      [rplus,cplus] = find(theta>theta(Nmax*fac/2+5,Nmax*fac/2+5+j)-.001↩
            & theta<theta(Nmax*fac/2+5,Nmax*fac/2+5+j)+.001);
71      kplus = length(rplus);
72      [rminus,cminus] = find(theta>theta(Nmax*fac/2+5,Nmax*fac/2+5+j)↩
           -.001+pi & theta<theta(Nmax*fac/2+5,Nmax*fac/2+5+j)+.001+pi);
73      kminus = length(rminus);
74
75      absrhoar = zeros(kminus+kplus+1,1);
76      zar = zeros(kminus+kplus+1,1);
77
78      for q = 1:kminus
79          zar(q) = -r(rminus(q),cminus(q));
80          absrhoar(q) = abs(rho(rminus(q),cminus(q)));
81      end
82
83      zar(kminus+1) = r(1025,1025);
84      absrhoar(q+1) = abs(rho(1025,1025));
85
86      for q = 1:kplus
87          zar(q+1+kminus) = r(rplus(q),cplus(q));
88          absrhoar(q+1+kminus) = abs(rho(rplus(q),cplus(q)));
89      end
90
91      [zar,sortindex] = sort(zar);
92      absrhoar = absrhoar(sortindex);
93
94      width(j+8) = fwhm(zar,absrhoar);
95  end
96
97  avwidth = sum(width)/16*2; %average FWHM
98
99   figure(1)
100  imagesc(xhatbig(1,:),xhatbig(1,:),abs(rho))
101  axis image
102  annotation('textbox',[.4 0.05 .4 .04],'LineStyle','none','String',['↩
        HWHM: ',num2str(avwidth,4),], 'FontSize',14)
```

## RMS

```
close all
clear all
clc

load parameters.mat
load toroidal/stir_and_hold/prop_groundstate_l=3.mat
load toroidal/stir_and_hold/FT_groundstate_l=3.mat

%%%%%%%%%%%%%%%%%%%%%%%%%%%%%%%%%%%%%%%%%%%%%%%%%%%%%%%%%%%%%%%%%%%%%%%%%%%%
% calculating the radius of the BEC
%%%%%%%%%%%%%%%%%%%%%%%%%%%%%%%%%%%%%%%%%%%%%%%%%%%%%%%%%%%%%%%%%%%%%%%%%%%%

psibar = psifft;
lambda = 3;
[Nmax,~] = size (psibar);
[Nx,~] = size(x);

%Choice of factor, depending on choice of psibar
%upper factor for psibar = psibar, lower factor for numerical FT

%factor = Nmax*pi*hbar*tbar/2/m/lambda^2/max(max(abs(x)))^2;
factor = Nmax/Nx;

%%%%%%%%%%%%%%%%%%%%%%%%%%%%%%%%%%%%%%%%%%%%%%%%%%%%%%%%%%%%%%%%%%%%%%%%%%%%
% calculating n,rho,new sized grid
%%%%%%%%%%%%%%%%%%%%%%%%%%%%%%%%%%%%%%%%%%%%%%%%%%%%%%%%%%%%%%%%%%%%%%%%%%%%

n = abs(psibar).^2;
rho = fftshift(fft2(n,256*8,256*8));
[xhatbig,yhatbig,~,~,dx,dy,~,~,~,~,~,~] = variables(max(max(abs(xhat))↩
    )*factor,max(max(abs(yhat)))*factor,256*8);

%%%%%%%%%%%%%%%%%%%%%%%%%%%%%%%%%%%%%%%%%%%%%%%%%%%%%%%%%%%%%%%%%%%%%%%%%%%%
% 2nd moment
%%%%%%%%%%%%%%%%%%%%%%%%%%%%%%%%%%%%%%%%%%%%%%%%%%%%%%%%%%%%%%%%%%%%%%%%%%%%

nav = sum(sum(abs(rho)))*dx*dy;
xav = sum(sum(abs(rho).*xhatbig))*dx*dy/nav;
yav = sum(sum(abs(rho).*yhatbig))*dx*dy/nav;
x2av = sum(sum(abs(rho).*xhatbig.^2))*dx*dy/nav;
y2av = sum(sum(abs(rho).*yhatbig.^2))*dx*dy/nav;

deltax = sqrt(x2av - xav^2);
deltay = sqrt(y2av - yav^2);
delta = sqrt(deltax^2 + deltay^2);


```

```
figure(1)
imagesc(xhatbig(1,:),xhatbig(1,:),abs(rho))
axis image
annotation('textbox',[.4 0.05 .4 .04],'LineStyle','none','String',['2nd momentum: ',num2str(delta,4),], 'FontSize',14)
```

### Kinetic Energy

```
close all
clear all
clc

load parameters.mat
load vortices/FT_vortices_2_l=3.mat

%%%%%%%%%%%%%%%%%%%%%%%%%%%%%%%%
% Setting up k-vector
%%%%%%%%%%%%%%%%%%%%%%%%%%%%%%%%

[Nmax,~] = size(kxar);
[kx,ky] = meshgrid(kxar,kyar);
[theta,kr] = cart2pol(kx,ky);

dk = abs(kxar(2)-kxar(1))*10;
N = round(max(max(abs(kxar)))/dk);

k1D = dk/2 :dk:max(max(abs(kxar)));

%%%%%%%%%%%%%%%%%%%%%%%%%%%%%%%%
% Calculating E,E0
%%%%%%%%%%%%%%%%%%%%%%%%%%%%%%%%

n = abs(psiffttau).^2;
E = zeros(N,1);
nk = zeros(N,1);

for j=1:N
    [r,c] = find(kr<dk*j & kr > dk*(j-1));
    for l = 1:length(r)
        nk(j) = n(r(l),c(l))+nk(j);
        E(j) = hbar^2/2/m*kr(r(l),c(l))^2*n(r(l),c(l))+E(j);
    end
end


figure(1)
loglog(k1D,E)
xlabel('k in \mum^{-1}','FontName','New Century Schoolbook','FontSize',14)
```

```
41 ylabel('E(k)','FontName','New Century Schoolbook','FontSize',14)
42 set(gca,'FontSize',14);
43 figure(2)
44 plot(k1D,nk)
45 xlabel('k in \mum^{-1}','FontName','New Century Schoolbook','FontSize'↩
       ,14)
46 ylabel('n(k)','FontName','New Century Schoolbook','FontSize',14)
47 set(gca,'FontSize',14);
```

## Appendix B

# DERIVATION OF THE SCALING LAW

The general equation of motion for a quasi two-dimensional BEC in a Harmonic Trap is:

$$i\hbar\partial_t\phi(\boldsymbol{\rho},t) = \left[-\frac{\hbar^2}{2m}\boldsymbol{\nabla}_{\mathrm{T}}^2 + \frac{m}{2}\omega^2(t)\rho^2 + U_2(N-1)\left|\phi(\boldsymbol{\rho},t)\right|^2\right]\phi(\boldsymbol{\rho},t) \tag{B.1}$$
$$\omega(t) = \omega_0\Theta(t_0-t),$$

As one can see, the potential gets turned off at time $t_0 = 0$ and the upper equation can be solved by the following **Ansatz**:

$$\phi_{\mathrm{lab}}(\tilde{\boldsymbol{\rho}},t) = \frac{1}{\lambda(t)}\exp\left(i\frac{m\tilde{\rho}^2\dot{\lambda}}{2\hbar\lambda}\right)\tilde{\phi}\left(\frac{\tilde{\boldsymbol{\rho}}}{\boldsymbol{\lambda}},\tau\right) \tag{B.2}$$

That leads us with $\boldsymbol{\rho} = \frac{\tilde{\boldsymbol{\rho}}}{\lambda(t)}$ to:

$$\partial_t\phi_{\mathrm{lab}} = \left(-\frac{\dot{\lambda}}{\lambda} + \frac{im\tilde{\rho}^2}{2\hbar}\left(\frac{\ddot{\lambda}}{\lambda} - \left(\frac{\dot{\lambda}}{\lambda}\right)^2\right)\right)\phi_{\mathrm{lab}} + \frac{1}{\lambda}\mathrm{e}^{\left(i\frac{m\tilde{\rho}^2\dot{\lambda}}{2\hbar\lambda}\right)}\left[\frac{\partial\tilde{\phi}}{\partial x}\frac{\partial x}{\partial t} + \frac{\partial\tilde{\phi}}{\partial y}\frac{\partial y}{\partial t} + \frac{\partial\tilde{\phi}}{\partial t}\right]$$

$$\frac{\partial x}{\partial t} = -\frac{\tilde{x}}{\lambda^2}\cdot\dot{\lambda} = -x\frac{\dot{\lambda}}{\lambda}$$

$$\rightarrow \partial_t\phi_{\mathrm{lab}} = \left(-\frac{\dot{\lambda}}{\lambda} + \frac{im\rho^2}{2\hbar}\left(\ddot{\lambda} - \left(\dot{\lambda}\right)^2\right)\right)\phi_{\mathrm{lab}} + \frac{1}{\lambda}\mathrm{e}^{\left(i\frac{m\tilde{\rho}^2\dot{\lambda}}{2\hbar\lambda}\right)}\left[-\frac{\dot{\lambda}}{\lambda}\boldsymbol{\rho}\cdot\boldsymbol{\nabla}_{\boldsymbol{\rho}} + \partial_t\right]\tilde{\phi}$$

$$\partial_{\tilde{x}}\phi_{\mathrm{lab}} = i\frac{m\dot{\lambda}}{2\hbar\lambda}2\tilde{x}\phi_{\mathrm{lab}} + \frac{\mathrm{e}^{\left(i\frac{m\tilde{\rho}^2\dot{\lambda}}{2\hbar\lambda}\right)}}{\lambda}\left[\frac{1}{\lambda}\frac{\partial\tilde{\phi}}{\partial x}\right]$$

$$\partial_{\tilde{x}}^2\phi_{\mathrm{lab}} = i\frac{m\dot{\lambda}}{2\hbar\lambda}2\phi_{\mathrm{lab}} + i\frac{2m\dot{\lambda}x}{\hbar\lambda}\frac{\mathrm{e}^{\left(i\frac{m\tilde{\rho}^2\dot{\lambda}}{2\hbar\lambda}\right)}}{\lambda}\frac{\partial\tilde{\phi}}{\partial x} + \left(i\frac{m\dot{\lambda}}{2\hbar\lambda}2\tilde{x}\right)^2\phi_{\mathrm{lab}} + \frac{\mathrm{e}^{\left(i\frac{m\tilde{\rho}^2\dot{\lambda}}{2\hbar\lambda}\right)}}{\lambda}\left[\frac{1}{\lambda^2}\frac{\partial^2\tilde{\phi}}{\partial x^2}\right]$$

$$\rightarrow \triangle\phi_{\mathrm{lab}} = \left(2i\frac{m\dot{\lambda}}{\hbar\lambda} - \left(\frac{m\dot{\lambda}}{\hbar}\right)^2\rho^2\right)\phi_{\mathrm{lab}} + \left(i\frac{2m\dot{\lambda}}{\hbar\lambda}\frac{\mathrm{e}^{\left(i\frac{m\tilde{\rho}^2\dot{\lambda}}{2\hbar\lambda}\right)}}{\lambda}\boldsymbol{\rho}\cdot\boldsymbol{\nabla}_{\boldsymbol{\rho}} + \frac{\mathrm{e}^{\left(i\frac{m\tilde{\rho}^2\dot{\lambda}}{2\hbar\lambda}\right)}}{\lambda^3}\boldsymbol{\nabla}_{\boldsymbol{\rho}}{}^2\right)\tilde{\phi}$$

The following discussion is true for the equation of motion of a BEC in a harmonic trap (B.2), or also for the equation of motion in a toroidal trap (if one chooses $B(t) = 0$ for the

harmonic trap). We get a new equation of motion:

$$i\hbar\partial_t\phi(\tilde{\boldsymbol{\rho}},t)=\left[-\frac{\hbar^2}{2m}\boldsymbol{\nabla}_{\mathrm{T}}^2+\frac{m}{2}\omega^2(t)\tilde{\rho}^2+B(t)\cdot\exp\left(-\frac{\tilde{\rho}^2}{w(t)^2}\right)+U_2(N-1)\left|\phi(\tilde{\boldsymbol{\rho}},t)\right|^2\right]\phi(\tilde{\boldsymbol{\rho}},t) \tag{B.3}$$

The additional term is a Gaussian laser beam, that, as shown in the following, is modulated while doing the expansion. In the end we would like to end up with an equation such as the following:

$$i\hbar\partial_\tau\tilde{\phi}(\boldsymbol{\rho},\tau)=\left[-\frac{\hbar^2}{2m}\boldsymbol{\nabla}_{\mathrm{R}}^2+\frac{m}{2}\omega_0^2\rho^2+B_0\cdot\exp\left(-\frac{\rho^2}{w_0^2}\right)+U_2(N-1)\left|\tilde{\phi}(\boldsymbol{\rho},\tau)\right|^2\right]\tilde{\phi}(\boldsymbol{\rho},\tau) \tag{B.4}$$

with $B_0$ and $w_0$ the parameters for the Gaussian beam prior to the expansion.
Plugging the calculated derivations into equation (B.3). And neglecting all factors that are the same of both sides for better readability, using $\omega(t)=0$ for $t>0$ and adding $0=\frac{1}{2}m\omega_0^2\left(\frac{\rho^2}{\lambda^2}-\frac{\rho^2}{\lambda^2}\right)$, we get:

$$i\hbar\left(i\frac{m\rho^2}{2\hbar}\ddot{\lambda}\lambda+\partial_t\right)\tilde{\phi}=-\frac{\hbar^2}{2m}\left(\frac{{\boldsymbol{\nabla}_{\boldsymbol{\rho}}}^2}{\lambda^2}+\frac{m}{2}\omega_0^2\frac{\rho^2}{\lambda^2}+B(t)\mathrm{e}^{-\frac{\rho^2\lambda^2}{w(t)^2}}+Ng\frac{|\tilde{\phi}|^2}{\lambda^2}-\frac{m}{2}\omega_0^2\frac{\rho^2}{\lambda^2}\right)\tilde{\phi} \tag{B.5}$$

Since we wanted to end up with eq. (B.4), one has to choose:

$$\partial_\tau=\lambda(t)^2\partial_t \qquad \ddot{\lambda}=\frac{\omega_0^2}{\lambda^3}$$

$$B_0=B(t)\lambda(t)^2 \qquad w_0=\frac{w(t)}{\lambda}$$

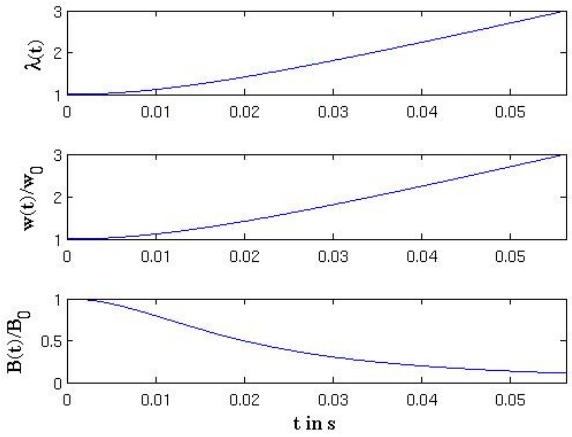


FIGURE B.1. The beam-parameters for different times t

# Appendix C

# THE DENSITY MATRIX

In Appendix C plots of the density matrices for all states used in this thesis are displayed.

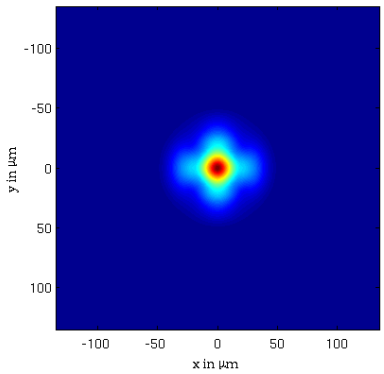


FIGURE C.1. Density matrix of state with 2 vortices

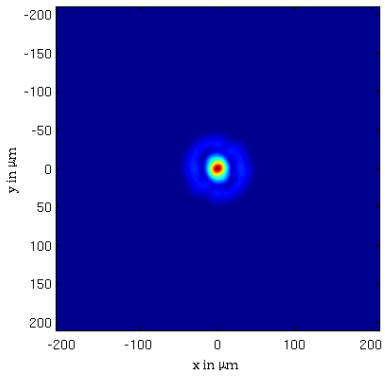


FIGURE C.2. Density matrix of state with 3 vortices

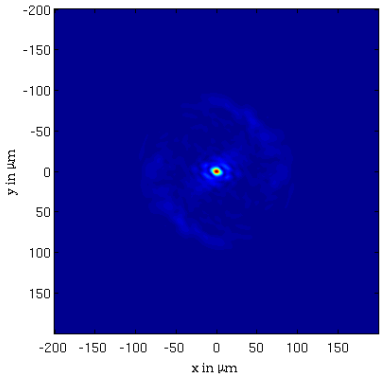


FIGURE C.3. Density Matrix of State originally in toroidal trap. After the creation of the vortices it was hold in this trap for $t_{\mathrm{hold}} = 1\ \mathrm{ms}$.

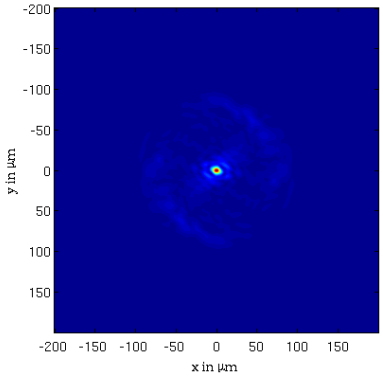


FIGURE C.4. Density Matrix of State originally in toroidal trap. After the creation of the vortices it was hold in this trap for $t_{\mathrm{hold}} = 51\ \mathrm{ms}$.

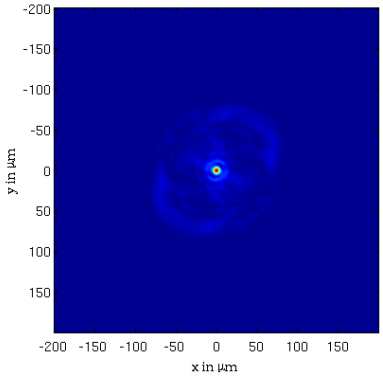


FIGURE C.5. Density Matrix of State originally in toroidal trap. After the creation of the vortices it was hold in this trap for $t_{\mathrm{hold}} = 1027\ \mathrm{ms}$.

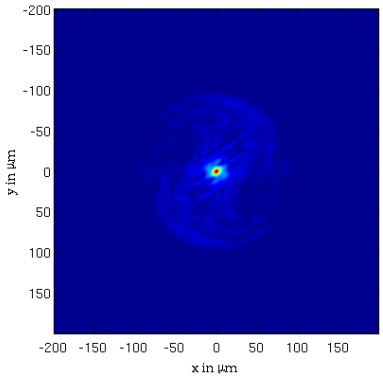


FIGURE C.6. Density Matrix of State originally in toroidal trap. After the creation of the vortices it was hold in this trap for $t_{\mathrm{hold}} = 5131\ \mathrm{ms}$.

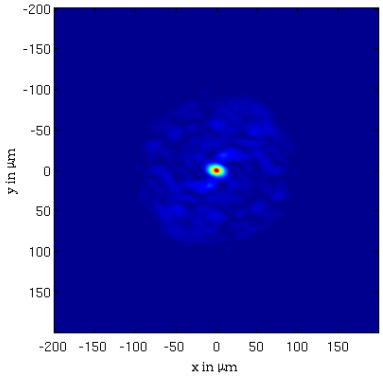


FIGURE C.7. Density Matrix of State originally in toroidal trap. After the creation of the vortices it was hold in this trap for $t_{\mathrm{hold}} = 6158\ \mathrm{ms}$.

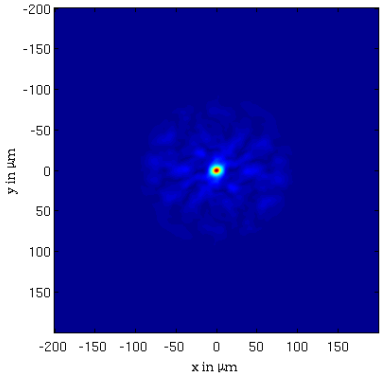


FIGURE C.8. Density Matrix of State originally in toroidal trap. After the creation of the vortices it was hold in this trap for $t_{\mathrm{hold}} = 10262\ \mathrm{ms}$.

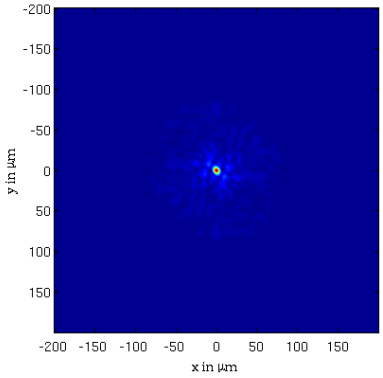


FIGURE C.9. Density Matrix of State originally in toroidal trap. After the creation of the vortices it was hold in this trap for $t_{\mathrm{hold}} = 14362\ \mathrm{ms}$.

# REFERENCES


[1] M.H. Anderson, J.R. Ensher, M.R. Matthews, C.E. Wieman, and E.A. Cornell. Observation of Bose-Einstein condensation in a dilute atomic vapor. Science, 269:198, 1995.

[2] C.C. Bradley, C.A. Sackett, J.J. Tollett, and R.G. Hulet. Evidence of Bose-Einstein condensation in an atomic gas with attractive interactions. Physical Review Letters, 1995.

[3] K.B. Davis, M.-O. Mewes, M.R. Andrews, N.J. van Druten, D.S. Durfee, D.M. Kurn, and W. Ketterle. Bose-Einstein condensation in a gas of sodium atoms. Physical Review Letters, 1995.

[4] A.H. van Amerongen et al. Yang-yang thermodynamics on an atom chip. Physical Review Letters, 2008.

[5] S. Tung, G. Lamporesi, D. Lobser, L. Xia, and E.A. Cornell. Observation of the presuperfluid regime in a two-dimensional bose gas. Physical Review Letters, 2010.

[6] I. Bloch, T.W. Hänsch, and T. Esslinger. Measurement of the spatial coherence of a trapped bose gas at the phase transition. Nature, 2000.

[7] C.J. Pethick and H. Smith. Bose-Einstein Condensation in Dilute Gases. Cambridge University Press, Cambridge, UK, 2002.

[8] W.H. Press, B.P. Flannery, S.A. Teukolsky, and W.T. Vetterling. Numerical Recipes - The Art of Scientific Computing. Press Syndicate of the University of Cambridge, 1986.

[9] M. Suzuki. Generalized trotter's formula and systematic approximants of exponential operators and inner derivations with applications to many-body problems. Communications in mathematical Physics, 51:183–190, 1976.

[10] T.W. Neely, E.C. Samson, A.S. Bradley, M.J. Davis, and B.P. Anderson. Observation of vortex dipoles in an oblate bose-einstein condensate. Physical Review Letters, 104(169401), 2010.

[11] Y. Castin and R. Dum. Bose-einstein condensates with vortices in rotating traps. The European Physical Journal D, March 1999.

[12] M. Naraschewski and R.J. Glauber. Spatial coherence and density correlations of trapped bose gases. Physical Review A, 1999.